Molecular Therapy
Nucleic Acids
Original Article

Effective gene therapy of Stargardt disease with PEG-ECO/*pGRK1-ABCA4-S/MAR* nanoparticles

Da Sun,[1,4] Wenyu Sun,[1,4] Song-Qi Gao,[1] Jonathan Lehrer,[1] Amirreza Naderi,[1] Cheng Wei,[1] Sangjoon Lee,[1] Andrew L. Schilb,[1] Josef Scheidt,[1] Ryan C. Hall,[1] Elias I. Traboulsi,[2] Krzysztof Palczewski,[3] and Zheng-Rong Lu[1]

[1]Department of Biomedical Engineering, Case Western Reserve University, 10900 Euclid Avenue, Cleveland, OH 44106, USA; [2]Department of Pediatric Ophthalmology and Center for Genetic Eye Diseases, Cole Eye Institute, Cleveland Clinic, 9500 Euclid Avenue, Cleveland, OH 44106, USA; [3]Gavin Herbert Eye Institute, Department of Ophthalmology, Departments of Physiology and Biophysics, Chemistry, and Molecular Biology and Biochemistry, University of California Irvine, Irvine, CA 92697, USA

Stargardt disease (STGD) is the most common form of inherited retinal genetic disorders and is often caused by mutations in *ABCA4*. Gene therapy has the promise to effectively treat monogenic retinal disorders. However, clinically approved adeno-associated virus (AAV) vectors do not have a loading capacity for large genes, such as *ABCA4*. Self-assembly nanoparticles composed of (1-aminoethyl)iminobis[N-(oleoylcysteinyl-1-amino-ethyl)propionamide (ECO; a multifunctional pH-sensitive/ionizable amino lipid) and plasmid DNA produce gene transfection comparable with or better than the AAV2 capsid. Stable PEG-ECO/*pGRK1-ABCA4-S/MAR* nanoparticles produce specific and prolonged expression of ABCA4 in the photoreceptors of *Abca4*$^{-/-}$ mice and significantly inhibit accumulation of toxic A2E in the eye. Multiple subretinal injections enhance gene expression and therapeutic efficacy with an approximately 69% reduction in A2E accumulation in *Abca4*$^{-/-}$ mice after 3 doses. Very mild inflammation was observed after multiple injections of the nanoparticles. PEG-ECO/*pGRK1-ABCA4-S/MAR* nanoparticles are a promising non-viral mediated gene therapy modality for STGD type 1 (STGD1).

INTRODUCTION

Inherited retinal diseases (IRDs) as a group are one of the main causes for vision impairment and blindness. Stargardt disease (STGD), the most common form of IRD, is characterized by reduction of central vision and visual acuity starting, in some cases, as early as the first decade of life and in others in early, mid-, or late adulthood.[1,2] The majority of individuals with STGD are diagnosed with type 1 STGD (STGD1), which is caused by mutations in the *ABCA4* gene (6.8 kb) encoding a 210-kDa ATP-dependent flippase importer.[3] Mutated ABCA4 loses its normal function of transporting toxic all-*trans*-retinal conjugates across disc membranes, resulting in accumulation of toxic bis-retinoids, including N-retinylidene-N-retinylethanolamine (A2E), and deposition of lipofuscin in the retinal pigment epithelium (RPE), which eventually causes retinal degeneration and vision loss.[4]

In one form of gene therapy, the mutated gene is replaced with a functional copy in the target cells. This therapeutic modality has shown a great promise to preserve and rescue vision in individuals with monogenic retinal disorders.[5,6] Gene therapy requires efficient delivery of plasmid DNA encoding a wild-type or functional gene into target cells to rescue or restore the gene's normal function. So far, adeno-associated virus (AAV)-based gene therapy is the only one that has been approved for treating type 2 Leber's congenital amaurosis (LCA2).[7] However, the small cargo capacity of AAV vectors limits their use for delivering larger genes and treatments for their associated diseases, such as the *ABCA4* gene.[8] Although adenoviruses and lentiviruses are able to deliver larger genes, immunogenicity and unintended side effects hinder their use in clinical trials.[9–11]

We have recently developed lipid nanoparticle-based gene therapy using a pH-sensitive amino lipid, ECO ((1-aminoethyl)iminobis[N-(oleoylcysteinyl-1-amino-ethyl)propionamide]), which self-assembles with nucleic acids of any size to form stable nanoparticle formulations without the need of helper lipids. After endocytosis of the nanoparticles, ECO facilitates pH-sensitive amphiphilic endosomal escape, followed by reductive cytosolic release (the PERC effect), resulting in efficient intracellular delivery of the therapeutic gene cargo.[12–18] ECO/DNA can be readily modified by PEGylations through controlled conjugation to a small fraction of the thiol groups on ECO. The effectiveness of ECO/DNA nanoparticles for *in vivo* delivery of therapeutic genes has been demonstrated previously in *Rpe65*$^{-/-}$ mice for treating LCA2 and in *Abca4*$^{-/-}$ mice for treating STGD1, respectively.[12,18,19] ECO/DNA nanoparticles have demonstrated an excellent safety profile after subretinal injection in mice. However, the *ABCA4* plasmid constructs used in the previous studies contained a bovine *RHO* promoter and a viral *SV40* enhancer, which were insufficient to produce the expected prolonged gene expression

Received 27 March 2022; accepted 17 August 2022;
https://doi.org/10.1016/j.omtn.2022.08.026.

[4]These authors contributed equally

Correspondence: Zheng-Rong Lu, PhD, Department of Biomedical Engineering, Case Western Reserve University, Wickenden 427, Mail Stop 7207, 10900 Euclid Avenue, Cleveland, OH 44106, USA.
E-mail: zxl125@case.edu

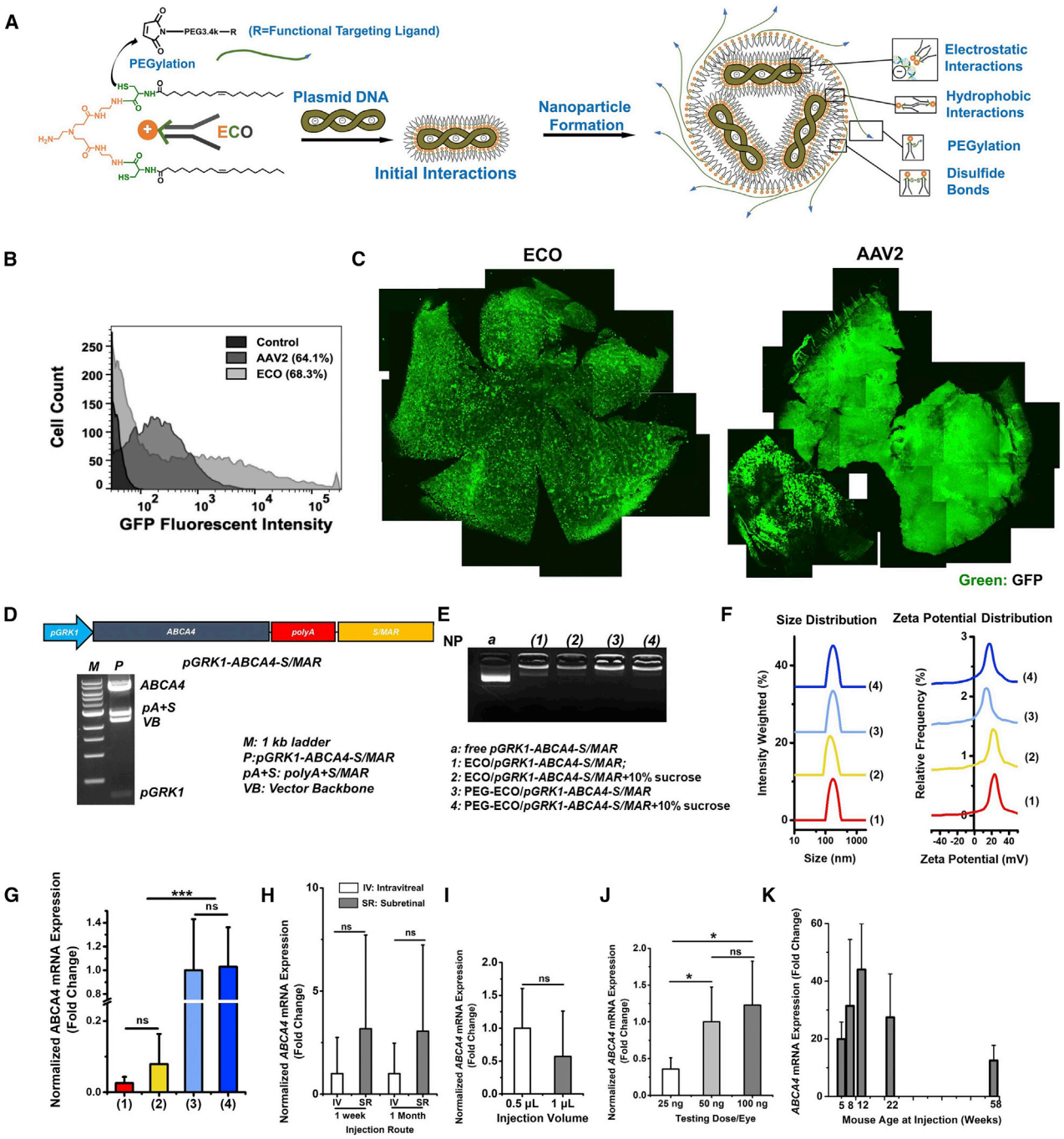

Figure 1. Formulation and characterization of ECO plasmid DNA nanoparticles

(A) Schematic of self-assembly formulation of ECO/plasmid DNA nanoparticles. (B and C) Flow cytometry histograms of GFP expression in ARPE-19 cells 48 h after transfection with EM-PEG-ECO/*pCMV-GFP* and AAV2-CMV-GFP (B) and fluorescence images of retinal flat mounts of GFP expression in BALB/c mice 4 months after a subretinal injection of EM-PEG-ECO/*pCMV-GFP* and AAV2-CMV-GFP (C). (D) Diagram of the therapeutic *pGRK1-ABCA4-S/MAR* plasmid construct and confirmation of the structure by restriction enzyme digestion agarose gel electrophoresis. (E and F) Characterization of different ECO/*pGRK1-ABCA4-S/MAR* nanoparticle formulations by agarose gel electrophoresis (E) and DLS of size and zeta potential distribution (F). (G) qRT-PCR of *ABCA4* mRNA expression in *Abca4*$^{-/-}$ mice 1 week after subretinal treatment with (1) ECO/*pGRK1-ABCA4-S/MAR*, (2) ECO/*pGRK1-ABCA4-S/MAR* (10% sucrose), (3) PEG-ECO/*pGRK1-ABCA4-S/MAR*, and (4) PEG-ECO/*pGRK1-ABCA4-*

(legend continued on next page)

and inhibition of A2E accumulation after a single subretinal injection in *Abca4*$^{-/-}$ mice.[12,18,19] It has also been reported that a scaffold/matrix attachment region (S/MAR) containing AT-rich regions can enhance a sustained long-term gene expression in retinal gene therapy.[20] We hypothesized that the design of an *ABCA4* plasmid containing a photoreceptor-specific promotor and an enhancer of human origin would result in prolonged gene expression and effective inhibition of A2E accumulation with the ECO based non-viral gene therapy and repeated administration of the ECO/DNA nanoparticles would significantly enhance the gene expression and therapeutic efficacy.

In this study, we designed and constructed a *ABCA4* plasmid (*pGRK1-ABCA4-SMAR*) with a G protein-coupled receptor kinase 1 (*GRK1*) promoter[21] and a *S/MAR* enhancer[20,22] of human origin. A stable PEG-ECO/*pGRK1-ABCA4-SMAR* nanoparticle formulation was developed as a clinically translatable gene therapy for STGD1. The gene expression, inhibition of A2E accumulation, and safety of the nanoparticles were investigated in *Abca4*$^{-/-}$ mice after single and multiple subretinal treatments.

RESULTS

Formulation and characterization of ECO plasmid DNA nanoparticles

The stepwise self-assembly formulation of PEGylated ECO/DNA nanoparticles is depicted in Figure 1A. PEG-maleimide or functionalized PEG-maleimide (2.5 mol %) first reacted with ECO for 30 min and was then mixed with plasmid DNA for another 30 min with agitation. An emixustat (EM)-functionalized PEGylated ECO/*pCMV-GFP* nanoparticle formulation (EM-PEG-ECO/*pCMV-GFP*) was prepared to compare its transfection efficiency with the AAV, using GFP as a reporter gene. EM-PEG-ECO/*pCMV-GFP* resulted in a higher transfection proportion than AAV2-*CMV-GFP* (68.3% versus 64.1%) and more cell populations with higher GFP expression levels in ARPE-19 cells 48 h after transfection (Figure 1B). Subretinal injection of EM-PEG-ECO/*pCMV-GFP* into BALB/c mice produced strong and well-dispersed GFP expression, as shown by confocal microscopy images of flat-mount retinal specimens 4 months after injection (Figure 1C). Significant GFP expression was also observed in the retina of mice injected with AAV2-CMV-GFP at the same DNA copy number. The ECO-based non-viral system provides gene transfection comparable with or better than the AAV and induces minimal inflammation in the eye.

The *pGRK1-ABCA4-S/MAR* plasmid was constructed for specific expression of ABCA4 in cone and rod photoreceptors (Figure 1D).[23–26] The *GRK1* promoter was inserted into *MluI* and *AgeI* restriction sites, and the human β-globin poly(A) and *S/MAR* DNA was inserted into *NotI* and *NheI* restriction sites. The plasmid structure was confirmed by agarose gel electrophoresis of selective digestion reactions at different restriction sites, where the *ABCA4* fragment (6.8 kb) was separated from the vector backbone (VB) and poly(A) and *SMAR* fragments (Figures 1D and S1B). The *pGRK1-ABCA4-S/MAR* plasmid (11.6 kb) was also verified by full-length sequencing. The therapeutic plasmid had *ABCA4* expression similar to *pRHO-ABCA4* in *Abca4*$^{-/-}$ mice (Figure S1C). Inclusion of the *S/MAR* enhancer resulted in prolonged *ABCA4* expression for more than 1 month compared with *pGRK1-ABCA4* (without the enhancer) in *Abca4*$^{-/-}$ mice (Figure S1D).

ECO formed stable nanoparticles with *pGRK1-ABCA4-S/MAR* under different conditions, as shown by agarose gel electrophoresis (Figure 1E). PEGylated nanoparticles were designed to sequester the positive charges of the core ECO/DNA nanoparticles and facilitate distribution across the retina for more efficient gene delivery in the retina. Sucrose (10%) was used as an excipient to improve the stability of the formulation for long-term storage. All nanoparticle formulations had a uniform size distribution (150–200 nm), and the PEGylated nanoparticles showed lower zeta potentials than the un-PEGylated nanoparticles (∼15 versus 22 mV) (Figure 1F; Table S1). The PEG-ECO/*pGRK1-ABCA4-S/MAR* formulation with 10% sucrose maintained excellent stability during storage at 4°C or −20°C for up to 1 month (Figure S2; Table S1). PEG-ECO/*pGRK1-ABCA4-S/MAR* nanoparticles showed much higher *ABCA4* mRNA expression than the un-PEGylated formulations in *Abca4*$^{-/-}$ mice 1 week after subretinal injection (Figure 1G). Excipient sucrose did not affect *ABCA4* mRNA expression for the PEGylated nanoparticle formulation (Figure 1G). Significant transfection efficiency was retained for the formulation after storage at −20°C for 70 days (Figure S2E).

We next investigated the effect of injection route, injection volume, dose, and age on gene transfection of PEG-ECO/*pGRK1-ABCA4-S/MAR* nanoparticles in *Abca4*$^{-/-}$ mice. PEG-ECO/*pGRK1-ABCA4-S/MAR* nanoparticles were tested by intravitreal and subretinal injections at the same dose and volume. Subretinal injection appeared to provide somewhat better transfection efficacy than intravitreal injection after 1 week and 1 month, but that difference was not statistically significant (Figure 1H). Intravitreal administration of PEG-ECO/*pGRK1-ABCA4-S/MAR* could also induce substantial *ABCA4* mRNA expression in the retina, suggesting the potential of the ECO-based nanoparticles for intravitreal administration. For subretinal injection, a small injection volume (0.5 μL) appeared to be favorable for high *ABCA4* mRNA expression compared with a large volume (1 μL) at the same DNA dose in the mouse model (Figure 1I). *ABCA4* mRNA expression was observed for all tested doses at the same injection volume (0.5 μL). However, a higher dose (100 ng/eye) resulted in higher *ABCA4* mRNA expression (Figure 1J). The age of the *Abca4*$^{-/-}$ mice did not have a significant effect on

S/MAR (10% sucrose). The mRNA expressions were normalized to that by PEG-ECO/*pGRK1-ABCA4-S/MAR*. (H–K) Characterization of *in vivo* gene expression of PEG-ECO/*pGRK1-ABCA4-S/MAR* in *Abca4*$^{-/-}$ mice with different injection routes (intravitreal versus subretinal) (H), injection volume (0.5 or 1 μL, expression normalized to 0.5 μL) (I), injection dose (25, 50, or 100 ng/eye, expression normalized to 50 ng/eye) (J), and age at treatment (K). Analyses were done by qRT-PCR of *ABCA4* mRNA expression 1 week or 1 month, as indicated, after single treatment of nanoparticles (100 ng/eye, 0.5 μL). *$p < 0.05$, **$p < 0.01$, ***$p < 0.005$.

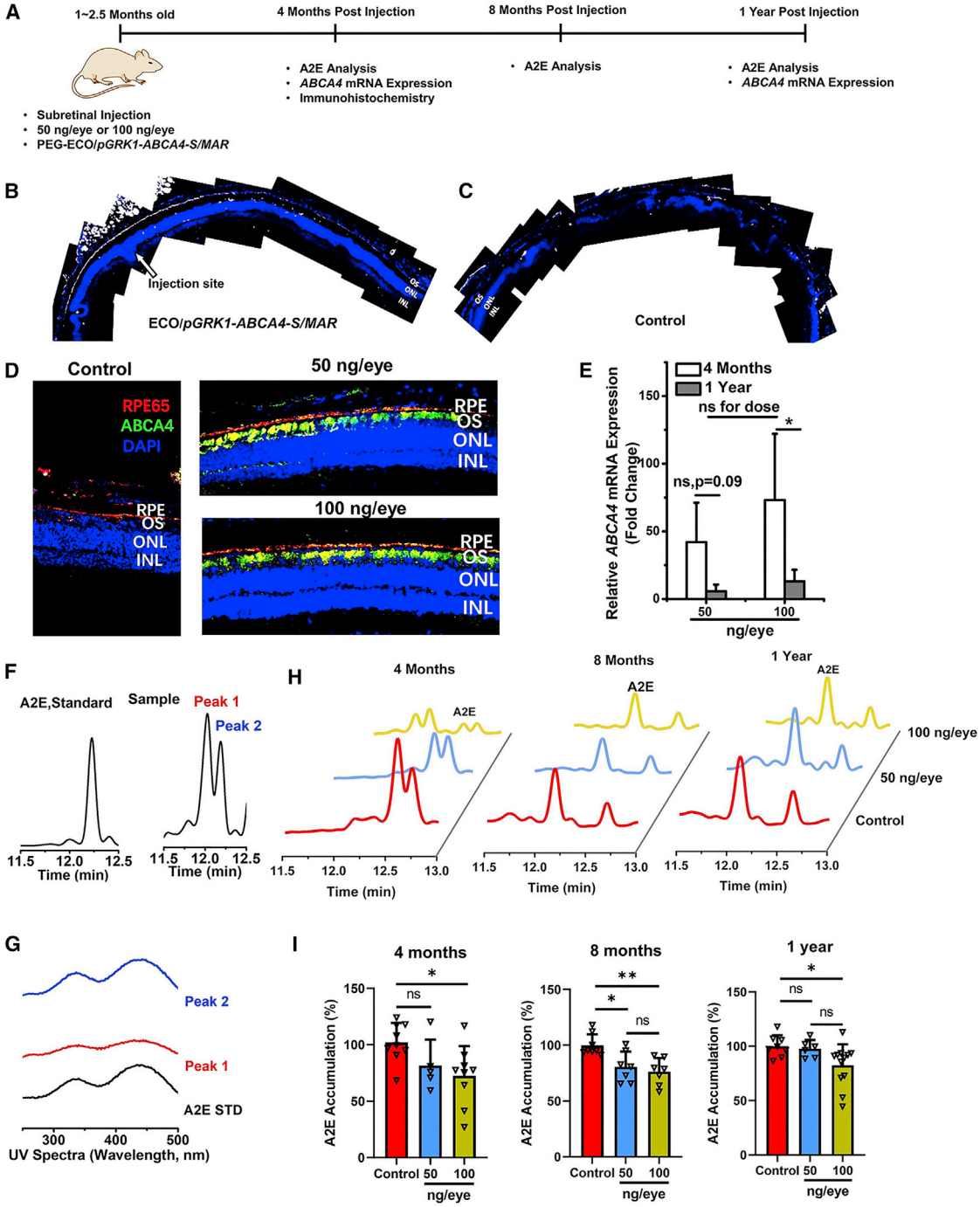

Figure 2. Treatment efficacy after a single dose of 50 ng or 100 ng/eye with PEG-ECO/*pGRK1-ABCA4-S/MAR* nanoparticles in *Abca4*$^{-/-}$ mice

(A) Timeline of treatment with PEG-ECO/*pGRK1-ABCA4-S/MAR* in *Abca4*$^{-/-}$ mice. (B and C) ABCA4 expression distribution in the retina of *Abca4*$^{-/-}$ mice after subretinal treatment with ECO/*pGRK1-ABCA4-S/MAR* nanoparticles (200 ng/μL, 1 μL) (B) and PBS (C) for 7 days. Analysis was conducted on confocal images of immunohistochemistry (IHC) staining with an ABCA4 antibody (ABCA4 expression is shown in white). (D) Fluorescence IHC staining of ABCA4 in the retina (red, RPE65; green, ABCA4; blue, DAPI) of *Abca4*$^{-/-}$ mice 4 months after a single treatment of PBS and PEG-ECO/*pGRK1-ABCA4-S/MAR* (50 ng or 100 ng/eye). (E) qRT-PCR of *ABCA4* mRNA expression in *Abca4*$^{-/-}$ mice 4 months and 1 year after treatment. (F and G) HPLC chromatograms (F) and UV spectra (G) of the A2E standard and A2E from eye samples of

(legend continued on next page)

ABCA4 mRNA expression. Robust *ABCA4* mRNA expression was observed in all tested age groups (5, 8, 12, 22 and 58 weeks old) 1 week after subretinal injection. A slight reduction (not significant) in *ABCA4* mRNA expression was observed in 58-week-old mice (Figure 1K).

Treatment efficacy after a single dose of PEG-ECO/*pGRK1-ABCA4-S/MAR* nanoparticles in *Abca4*$^{-/-}$ mice

Gene transfection of PEG-ECO/*pGRK1-ABCA4-S/MAR* nanoparticles was evaluated in *Abca4*$^{-/-}$ mice up to 1 year after a single subretinal injection, as shown in Figure 2A. Immunohistochemistry staining of ABCA4 protein revealed that PEG-ECO/*pGRK1-ABCA4-S/MAR* could facilitate a relatively broad distribution of ABCA4 expression in the retina, where clear ABCA4 expression (white color) in the outer segments (OSs) at and away from the injection site was observed (Figure 2B). Expression faded at the location farther away from the injection site, and no expression was observed from the control (Figure 2C). Substantial ABCA4 expression in the OS (green) was observed 4 months after a single subretinal injection at doses of 50 and 100 ng/eye (Figure 2D). Expression was also observed in the RPE, possibly because of phagocytosis of OSs shed by the photoreceptors in the RPE. Expression of *ABCA4* was also evaluated at the mRNA level by qRT-PCR. Robust expression of *ABCA4* mRNA was observed for both doses at 4 months, but expression faded 1 year after a single dose (Figure 2E).

Therapeutic efficacy was determined by analyzing inhibition of A2E accumulation in *Abca4*$^{-/-}$ mice. A2E, a dimer of vitamin A, is the main component in lipofuscin and can induce phototoxic events.[27,28] A2E is widely accepted as an indicator of STGD1 progression.[29] One of the treatment strategies for STGD1 is to minimize A2E production and chronic oxidative damage-induced atrophy.[30] A2E accumulation has been shown to increase gradually in *Abca4*$^{-/-}$ mice with age.[18,19] A2E accumulation was analyzed using HPLC, where the A2E peak was identified from chromatograms with the same elution time as an A2E standard (Figure 2F). A2E sometimes appeared as 2 peaks in the chromatograms with similar UV spectra (Figures 2F and 2G), suggesting that they are geometric isomers of retinal moiety. Reduction of A2E accumulation was observed from the HPLC chromatograms of the eye extracts of *Abca4*$^{-/-}$ mice treated with a single dose (50 or 100 ng/eye) of PEG-ECO/*pGRK1-ABCA4-S/MAR* after 4, 8, and 12 months, as demonstrated by the reduced size of the A2E peaks compared with the control (Figure 2H). Quantitative analysis revealed an 18.5% reduction of A2E accumulation at the 50 ng/eye dose of therapeutic DNA and 32% at the 100 ng/eye at 4 months compared with the control, 9.5% for 50 ng/eye and 24.7% for 100 ng/eye at 8 months, and 2.4% for 50 ng/eye and 17.4% for 100 ng/eye after 1 year (Figure 2I). The high dose (100 ng/eye) resulted in a more substantial and prolonged reduction of A2E accumulation after a single dose compared with the effect of the low dose (50 ng/eye), consistent with the duration of gene transfection.

Gene expression and therapeutic efficacy of repeated dosing of PEG-ECO/*pGRK1-ABCA4-S/MAR* nanoparticles in *Abca4*$^{-/-}$ mice

A multi-dosing strategy was explored next to enhance prolonged gene expression and therapeutic efficacy of PEG-ECO/*pGRK1-ABCA4-S/MAR*. The timeline of multi-treatment schedules in *Abca4*$^{-/-}$ mice is illustrated in Figure 3A. To properly compare gene expression and efficacy of different dosing strategies, mice that received 1 injection were sacrificed 8 months after injection, mice that received 2 injections were sacrificed 5 months after the last injection (8 months after the initial treatment), and that mice received 3 injections were sacrificed 5 months after the last injection. As shown in Figure 3B, *ABCA4* mRNA expression decayed over time after a single injection of PEG-ECO/*pGRK1-ABCA4-S/MAR* nanoparticles (100 ng/eye) in *Abca4*$^{-/-}$ mice. Based on this result, we performed multiple injections of PEG-ECO/*pGRK1-ABCA4-S/MAR* every 3 months. ABCA4 protein expression in the retina of *Abca4*$^{-/-}$ mice after 1, 2, and 3 injections was evaluated by immunohistochemistry (IHC) staining. ABCA4 expression increased with the number of treatments, as indicated by an increased green signal in the OS of the retina of *Abca4*$^{-/-}$ mice (Figure 3C). After 3 treatments, ABCA4 expression was observed in more than 70% of the retina (Figure 3D). A considerable amount of ABCA4 protein was detected in the RPE layer, as indicated by the yellow color because of overlap of the red fluorescence staining of RPE65 and green fluorescence staining of ABCA4. At the mRNA level, substantially more *ABCA4* mRNA expression was observed for mice that received 3 treatments compared with 1 or 2 treatments (Figure 3E). However, there was no significant difference in *ABCA4* mRNA expression between double dosing and single dosing. Because protein has a longer half-life than mRNA, ABCA4 protein expression was significantly higher for 2 treatments than for 1 treatment.

Repeated injections also resulted in significantly more inhibition of A2E accumulation in *Abca4*$^{-/-}$ mice. The HPLC chromatograms (Figures 3F and S6) showed the reduced size of the A2E peaks in *Abca4*$^{-/-}$ mice that received 1, 2, or 3 injections compared with controls. Quantitative analysis revealed about 13.7% inhibition of A2E accumulation after 1 treatment, 30% after 2 treatments, and 69% after 3 injections, demonstrating significantly enhanced therapeutic efficacy of multiple injections (Figure 3G). The multi-treatments could slow down accumulation of A2E in the retina, but they would not reduce the amount of A2E that had already accumulated in the retina, which could be observed from quantification of the A2E amount in the retina (Figure S7). The multiple-injections protocol for PEG-ECO/*pGRK1-ABCA4-S/MAR* produced a high level of prolonged expression of ABCA4, resulting in robust inhibition of A2E accumulation, which is indicative of effective treatment of STGD1.

1-year old *Abca4*$^{-/-}$ mice, where the A2E peak was identified with the same elution time as the A2E standard. (H and I) Representative HPLC chromatograms of A2E (H) and the A2E levels quantified from HPLC relative to the control (I) 4, 8, and 12 months after a single treatment with PEG-ECO/*pGRK1-ABCA4-S/MAR* (50 ng or100 ng/eye) in *Abca4*$^{-/-}$ mice (*$p < 0.05$, **$p < 0.01$).

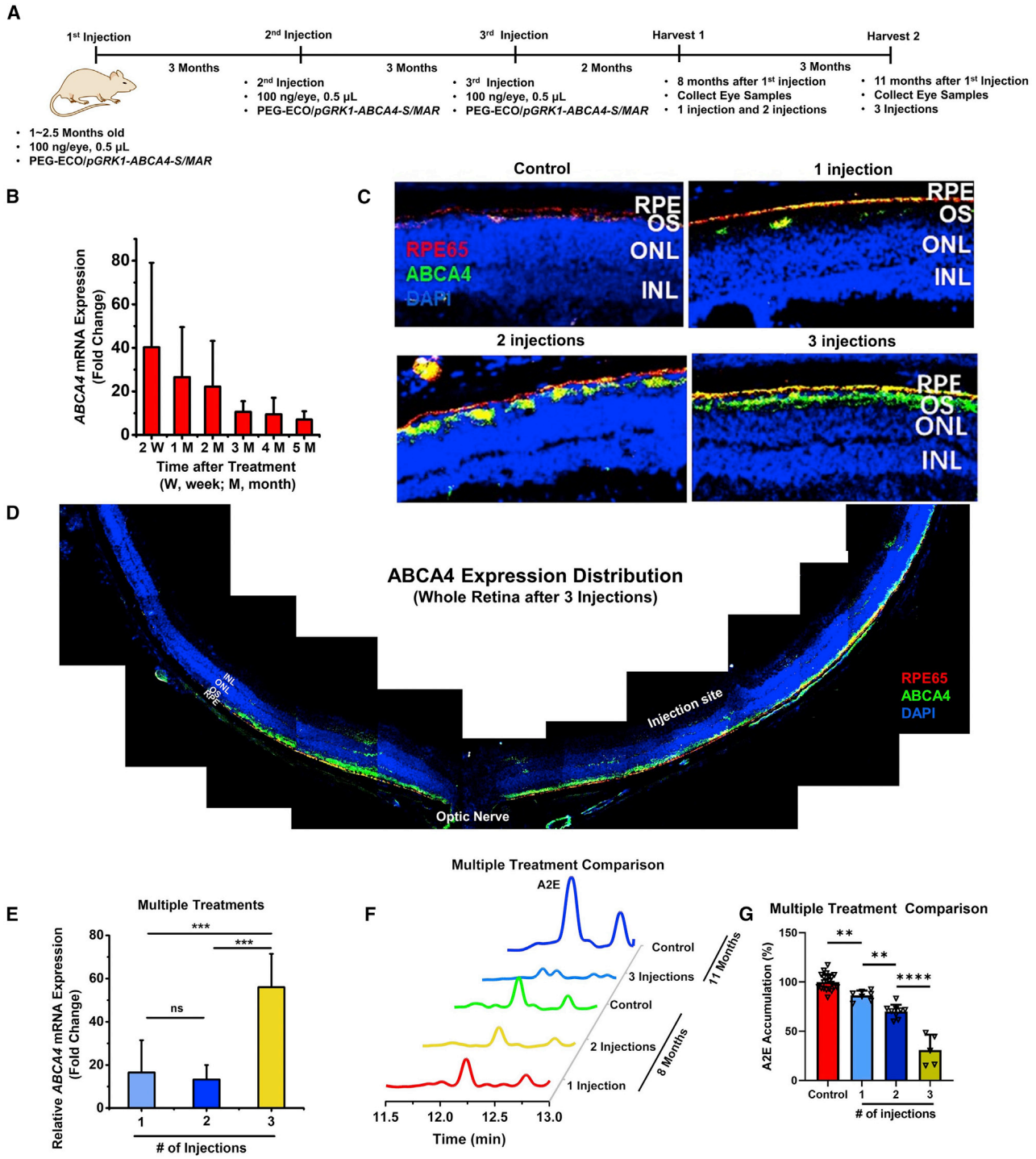

Figure 3. Gene expression and therapeutic efficacy of repeated dosing of PEG-ECO/*pGRK1-ABCA4-S/MAR* nanoparticles in *Abca4*$^{-/-}$ mice

(A) Timeline of repeated injections of PEG-ECO/*pGRK1-ABCA4-S/MAR* nanoparticles. (B) Time course of *ABCA4* mRNA expression, analyzed by qRT-PCR after 1 injection of PEG-ECO/*pGRK1-ABCA4-S/MAR* nanoparticles (100 ng/eye) in *Abca4*$^{-/-}$ mice. (C and D) Fluorescence IHC staining of ABCA4 (green) and RPE65 (red) of retina sections from *Abca4*$^{-/-}$ mice that received 1, 2, and 3 subretinal injections of PEG-ECO/*pGRK1-ABCA4-S/MAR* (100 ng/eye; blue, DAPI) (C) and of the whole retina after 3 injections (D). (E) qRT-PCR of *ABCA4* mRNA expression in *Abca4*$^{-/-}$ mice that received 1, 2, and 3 injections of PEG-ECO/*pGRK1-ABCA4-S/MAR*. (F) Representative HPLC chromatograms of A2E in the eyes of *Abca4*$^{-/-}$ mice treated with PEG-ECO/*pGRK1-ABCA4-S/MAR* nanoparticles in comparison with that in control mice. (G) Quantitative comparison of A2E levels in treated *Abca4*$^{-/-}$ mice relative to control mice. *$p < 0.05$, **$p < 0.01$, ***$p < 0.005$, ****$p < 0.001$.

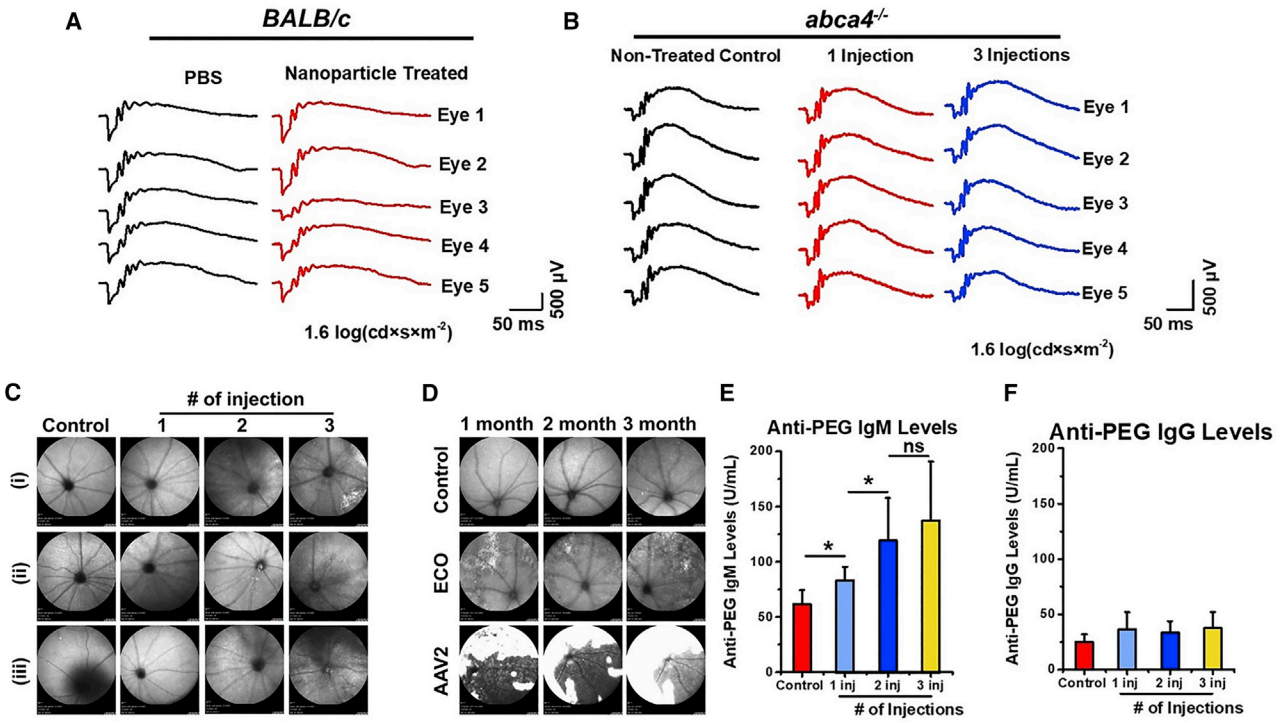

Figure 4. Safety of subretinal injection of PEG-ECO/*DNA* nanoparticles

(A and B) Scotopic electroretinogram (ERG) responses of BALB/c mice 1 month after subretinal injection of ECO/*pGRK1-ABCA4-S/MAR* nanoparticles (A) and of *Abca4*$^{-/-}$ mice 10–10.5 months after subretinal injection of a single dose (100 ng/eye) or 3 doses (every 3 months, 100 ng/eye) of PEG-ECO/*pGRK1-ABCA4-S/MAR* nanoparticles (B) at a test light intensity of 1.6 log(cd × s × m^{-2}). (C) Eye morphology, demonstrated by scanning laser ophthalmoscopy (SLO), of *Abca4*$^{-/-}$ mice that received multiple treatments of PEG-ECO/*pGRK1-ABCA4-S/MAR* nanoparticles 7 months after the initial treatment (control, untreated). (D) Eye morphology (SLO) of BALB/c mice treated with EM-PEG-HZ-ECO/*pCMV-GFP* nanoparticles and AAV2-CMV-GFP (dose, 5 × 10^9 gene copies; control, untreated) 1, 2, and 3 months after treatment (large white area, potential inflammation). (E and F) PEG antibody analysis of anti-PEG IgM (E) and anti-PEG IgG (F) levels from the blood of *Abca4*$^{-/-}$ mice that received multiple treatments of PEG-ECO/*pGRK1-ABCA4-S/MAR* nanoparticles. *p < 0.05, **p < 0.005, ****p < 0.0001.

Safety of subretinal injection of PEG-ECO/*DNA* nanoparticles

The safety of PEG-ECO/*pGRK1-ABCA4-S/MAR* was evaluated *in vitro* and *in vivo* to assess cell toxicity, eye function, retinal morphology, and immunological response. PEG-ECO/*pGRK1-ABCA4-S/MAR* nanoparticles displayed no obvious cytotoxicity compared with un-PEGylated ECO/*pGRK1-ABCA4-S/MAR* (Figure S8). After a single injection of PEG-ECO/*pGRK1-ABCA4-S/MAR*, no change was observed in the scotopic electroretinogram (ERG) responses from BALB/c mice 1 month after treatment (Figure 4A and S9). There was also no change observed in scotopic ERG responses in *Abca4*$^{-/-}$ mice receiving a single treatment or multiple treatments (3 injections) of PEG-ECO/*pGRK1-ABCA4-S/MAR* (Figures 4B and S10). Eye morphology was evaluated using scanning laser ophthalmoscopy (SLO) with *Abca4*$^{-/-}$ mice receiving one or multiple treatments of PEG-ECO/*pGRK1-ABCA4-S/MAR* nanoparticles. SLO was performed 7 months after the initial treatment. SLO images (Figures 4C and S11) did not show any severe adverse effect associated with the treatments. Mild inflammation was present in some of the eyes of the *Abca4*$^{-/-}$ mice 1 month after the third injection of the nanoparticles (Figure S11). This inflammation might be caused by the invasive subretinal injection, and it could be alleviated later, as evidenced by clean SLO images of *Abca4*$^{-/-}$ mice 5 months after the second injection and 7 months after the single treatment (Figure S11). SLO was also used to compare EM-PEG-HZ-ECO/*pCMV-GFP* with AAV2. AAV2 seemed to induce more lesions and possible inflammation, as shown by the saturated white regions, than EM-PEG-HZ-ECO/*pCMV-GFP* (Figure 4D).

An antibody against PEG was also evaluated in mice that received PEG-ECO/*pGRK1-ABCA4-S/MAR* treatments. Compared with the control group, anti-PEG immunoglobulin M (IgM) levels were elevated in the treated groups, but at a relatively low level, which may not have a negative effect on the treatment, especially after multiple injections (Figure 4E). The anti-PEG IgG levels in the groups that received 1, 2, or 3 injections were slightly increased compared with the control group but not in a statistically significant fashion (Figure 4F). The results indicate that PEG-ECO/*pGRK1-ABCA4-S/MAR* nanoparticles may not elicit a significant immune response because of PEGylation. Overall, PEG-ECO/*pGRK1-ABCA4-S/MAR* nanoparticles demonstrated excellent safety compared with the AAV.

DISCUSSION

We have been working on a clinically translatable, ECO-based, non-viral gene therapy for treating STGD1. In this work, based on observations of previously developed ECO/*ABCA4* plasmid nanoparticles, a therapeutic plasmid, *pGRK1-ABCA4-S/MAR*, with a human *GRK1* promoter and *S/MAR* enhancer was designed to achieve specific expression of ABCA4 protein in cone and rod photoreceptors. Significantly prolonged specific expression of ABCA4 was achieved with PEG-ECO/*pGRK1-ABCA4-S/MAR* nanoparticles in *Abca4*$^{-/-}$ mice, a STGD1 mouse model. The nanoparticles demonstrated an excellent safety profile. Repeated administration of the nanoparticles greatly enhanced gene expression and therapeutic efficacy. After 3 treatments within 1 year, A2E accumulation was reduced about 70% compared with controls. The PEG-ECO/*pGRK1-ABCA4-S/MAR* nanoparticles show great promise as a non-viral gene therapy for treating STGD1.

Currently, there is no approved therapy for treating STGD. However, several small-molecule drugs targeting the retinoid vision cycle or inhibiting lipofuscin accumulation in RPE cells are being or have been tested in clinical trials. EM is an oral drug that inhibits RPE65 protein and slows down the production and accumulation of toxic all-*trans*-retinal and bis-retinoids in the RPE. EM shows dose-dependent inhibition of RPE65 activity and delayed dark adaptation, consistent with the drug's mechanism of action.[31] C20-D3-vitamin A (ALK001) inhibits production of the vitamin A dimer A2E and subsequent lipofuscin accumulation, which can prevent vision loss in individuals with STGD1.[32] Remofuscin (or soraprazan) is an inhibitor of H^+/K^+ ATPase and is able to remove lipofuscin from the RPE. It has been shown to have low toxicity and holds promise for local treatment of STGD1 in *Abca4*$^{-/-}$ mice.[33]

Gene therapy corrects and restores the function of mutated genes and is therefore advantageous to treat monogenic inherited retinal disorders. Lentiviruses are capable of delivery and incorporation of relatively large therapeutic genes into the genome of transfected cells and provide stable, sustained gene expression. Subretinal injection into *Abca4*$^{-/-}$ mice of equine infectious anemia virus (EIAV)-derived lentiviral vectors (EIAV-lentivirus) loaded with the wild-type human *ABCA4* gene resulted in effective expression of ABCA4 protein in photoreceptor cells and significant reduction of A2E accumulation 1 year after a single treatment compared with untreated control mice.[34] Besides transient inflammation in animals, EIAV-lentivirus vectors are well tolerated.[35] However, no other reports are available regarding the progress and efficacy of lentivirus-based gene therapy in clinical trials.

AAVs exhibit low immunogenicity and the ability to diffuse and transfect various cell types in the retina. AAV-based gene therapy has been approved for treating individuals with LCA2.[7] Because of the large size of the *ABCA4* gene, dual AAV vectors encoding different sections of the *ABCA4* gene and multi-AAV vectors using an intein-mediated *trans*-splicing strategy have been used for recombinational expression of full-length ABCA4 protein in photoreceptors. The dual AAV vectors mediated substantial expression of full-length ABCA4 protein with reduced expression of truncated proteins and exhibited diminished A2E accumulation in *Abca4*$^{-/-}$ mice.[36,37] The intein-mediated *trans*-splicing strategy demonstrated full-length ABCA4 protein recombination and improvement of the STGD1 phenotype.[38] Clinical studies have shown that a single subretinal administration of AAV therapy improved the vision of individuals with LCA2, but retinal degeneration continued to progress.[39] The possibility of repeated administration of the AAV gene therapy remains tentative because of the concern that the immune response that follows the initial treatment could render the repeated treatment ineffective.[40]

Non-viral gene therapies for IRDs have gained increased attention because of their advantages of unlimited cargo capacity, ease of production, low cost, and better safety profile. Among non-viral gene delivery systems, lipid nucleic acid nanoparticles provide a versatile non-viral platform for efficient intracellular delivery of all types of nucleic acids, including small interfering RNA (siRNA), microRNA (miRNA), mRNA, and DNA, without cargo size limitation. Compared with viral vectors, lipid nanoparticles have shown excellent safety profiles and low immunogenicity, and they can be produced readily in a cost-effective way. Recently, lipid nanoparticle-based mRNA vaccines have been successfully used to combat severe acute respiratory syndrome coronavirus 2 (SARS-CoV-2) during the global pandemic of coronavirus disease 2019 (COVID-19).[41,42] Lipid nanoparticle-based gene therapy has the potential to be administered safely and repeatedly to efficiently treat human diseases caused by genetic malfunctions.

ECO is a multifunctional, pH-sensitive, ionizable amino-lipid platform for efficient delivery of therapeutic nucleic acids via local or systemic administration.[13–15,18,43–46] Its multifunctionality allows formulation of stable nanoparticles with small RNA or large plasmid DNA via self-assembly without helper lipids and enables the nanoparticles to sense and respond to environmental changes during the delivery process to achieve highly efficient cytosolic delivery of genetic materials. Specifically, ECO lipid nanoparticles remain stable at a physiological pH of 7.4. After being internalized through endocytosis, the lipids are protonated or ionized at pH 5.4–6.5, the endosomal pH, and acquire amphiphilicity, which induces endosomal membrane destabilization and promotes efficient endosomal escape into the cytosol. In the reductive cytoplasm, the disulfide crosslinks in the lipid nanoparticles undergo reductive cleavage, leading to nanoparticle dissociation and gene cargo release. The ECO/DNA nanoparticles can be readily modified by PEGylation or a targeting agent via a PEG spacer to minimize non-specific uptake and achieve specific delivery.[19] Upon subretinal injection, the targeted ECO/*pGFP* nanoparticles mediated comparable or better *in vitro* and *in vivo* gene transfection and minimal inflammation. A single injection of the nanoparticles could result in protein expression in the whole retina, indicating diffusion of the nanoparticles across the retina (Figure 1C).

A single subretinal injection of PEG-ECO/*pGRK1-ABCA4-S/MAR* at 100 ng/eye resulted in robust ABCA4 protein expression in

photoreceptors for at least 4 months and detectable expression and significant reduction of A2E accumulation 1 year after injection (Figures 2 and 3C). Kinetics analysis of mRNA expression after the single dose revealed gradual diminution of the *ABCA4* mRNA level over time (Figure 3B). Transfection efficiency and therapeutic efficacy were enhanced by repeated administration of PEG-ECO/*pGRK1-ABCA4-S/MAR*, which is an advantageous feature of non-viral gene therapy over viral therapies. Repeated injections at 3-month intervals greatly enhanced the prolonged robust expression of ABCA4 at the mRNA and protein levels in the retina and provided greater inhibition of A2E accumulation in the eye compared with the single and double treatments (Figure 3). The nanoparticles exhibited excellent safety, and no adverse effects were observed in retinal cells or in mouse eye function or morphology after multiple injections (Figure 4). The transient inflammation related to subretinal injection was alleviated soon after treatment with proper care, whereas significant inflammation caused by subretinal injection of the AAV lasted much longer under the same care conditions.

The *pGRK1-ABCA4-S/MAR* plasmid mediated specific expression in rod and cone photoreceptors. Specific gene expression in target cells would minimize off-target effects and also improve the safety of gene therapy.[47] The presence of ABCA4 protein was also observed in the RPE layer (Figures 2D and 3C). Because *pGRK1-ABCA4-S/MAR* only expresses in photoreceptors, the presence of ABCA4 in the RPE layer could be attributed to phagocytosis of OSs shed by photoreceptors in RPE cells. PEG-ECO/*pGRK1-ABCA4-S/MAR* also resulted in substantial ABCA4 mRNA expression after intravitreal injection, although subretinal injection resulted in slightly higher expression. Future studies will explore intravitreal injections of PEG-ECO/*pGRK1-ABCA4-S/MAR* for gene therapy of STGD1.

We have shown that PEG-ECO/*pGRK1-ABCA4-S/MAR* nanoparticles are an effective delivery mechanism to elicit specific expression of ABCA4 protein in photoreceptors. Repeated subretinal injections resulted in prolonged ABCA4 expression and enhanced therapeutic efficacy, with significant inhibition of A2E accumulation for effective treatment of STGD1. The nanoparticles exhibit an excellent safety profile with multiple subretinal injections, demonstrating no obvious adverse effect and little immunogenicity. Multifunctional, pH-sensitive, amino-lipid ECO is a promising platform for delivery of therapeutic genes without size limitation for gene therapy. PEG-ECO/*pGRK1-ABCA4-S/MAR* nanoparticles have the potential for clinical translation to treat STGD1.

MATERIALS AND METHODS

Reagents

All reagents were directly purchased from vendors and were used without further purification. Trifluoroacetic acid (TFA) was purchased from Oakwood Products (West Columbia, SC, USA). Methanol, methylene chloride (DCM), acetonitrile (ACN), and chloroform were obtained from Fisher Scientific (Hampton, NH, USA). For cell culture, fetal bovine serum, penicillin, and streptomycin were purchased from Invitrogen (Carlsbad, CA, USA). The plasmid for the reporter gene (*pCMV-GFP*) was purchased from Addgene (11,153). AAV2-CMV-GFP was purchased from Vector Biosystems (Malvern, PA, USA).

Cell culture

ARPE-19 cells were originally purchased from the ATCC (Manassas, VA, USA) and processed and sub-cultured following the vendor's protocol. Specifically, ARPE19-cells were maintained in Dulbecco's modified Eagle's medium (10% fetal bovine serum, 100 units/mL penicillin, and 100 μg/mL streptomycin) and cultured in a humidified incubator (37°C with 5% CO_2). The cells were passaged every 3 days at a 1:10 ratio.

Animals

Animals were housed and bred following an approved protocol (2014-0053, Case Western Reserve University Institutional Animal Care and Use Committee) in the Animal Resource Center, which was strictly in compliance with the recommendations of the American Veterinary Medical Association Panel on Euthanasia and the ARVO Statement for the Use of Animals involved in Ophthalmic and Vision Research. BALB/c mice (wild type) were obtained directly from Jackson Laboratory (Bar Harbor, ME, USA). *Abca4*$^{-/-}$ knockout mice (pigmented) were generated and maintained as described previously.[48]

Plasmid constructs

Plasmids were transformed using MAX Efficiency DH5α Competent *E. coli* (Life Technologies) and allowed to grow overnight on LB agar plates with ampicillin. Selected colonies were amplified, allowed to grow overnight, and then purified using a QIAGEN Maxi Kit. The purity and size of plasmid products were verified by gel electrophoresis. The *pGRK1-ABCA4-S/MAR* construct was created from the *pRHO-DsRed* plasmid (Addgene, 11156). First, *dsRed* was replaced with *ABCA4* between the restriction enzyme sites of *AgeI* and *NotI*. Then a *MluI* cutting site was introduced by site-directed mutagenesis in front of the bovine Rhodopsin promoter (*RHO*) before insertion of the *GRK1* promoter between the *MluI* and *AgeI* sites to replace *RHO*. Human β-globin poly(A) was introduced downstream of *ABCA4*, and the human *S/MAR* was inserted farther downstream. An *SpeI* cutting site was introduced between poly(A) and *S/MAR*.

Agarose gel electrophoresis

Agarose gels were prepared by heating 0.7%–2% agarose in 1× Tris borate-EDTA (TBE) buffer (Thermo Fisher Scientific, Waltham, MA, USA). Then 1 μL ethidium bromide (EtBr) was added per 50 mL of gel and poured into a mold for solidification. The tested plasmid samples were mixed with a 6× DNA-loading dye (New England Biolabs, Ipswich, MA, USA) before loading, and a 1-kb DNA ladder (New England Biolabs) was loaded to the leftmost lane. For cloning products, separation was effected by applying 80 V for 80 min, and for nanoparticle characterization, 120 V was applied for 25 min. All gels were imaged by a ChemiDoc XRS + gel imaging system (Bio-Rad, Hercules, CA, USA).

ECO/*pDNA* nanoparticle formulation

ECO was synthesized as described previously.[45,49] ECO/*pDNA* nanoparticles were formulated through self-assembly of the lipid ECO and plasmid DNA at an amine/phosphate (N/P) ratio of 8. For *in vitro* transfection, an ECO stock solution (2.5 mM in ethanol) and a plasmid DNA stock solution (0.5 mg/mL), at predetermined amounts based on the N/P ratio, were diluted to the same final volume with nuclease-free water. The mixture was then mixed on a vortex for 30 min at room temperature. For *in vivo* experiments, a different ECO stock solution (25 mM) was used. For PEGylated nanoparticles, ECO (2.5 mM in ethanol) and PEG-MAL (0.625 mM in water) or EM-PEG-HZ-MAL EM-modified targeting ligand (0.4 mM in water; 2.5 mol % of ECO) were first mixed and reacted in aqueous solution for 30 min. Then the mixture was added drop by drop, while vortexing for 30 min at room temperature, to the plasmid DNA (0.5 mg/mL) aqueous solution at a volume predetermined from the N/P ratio of 8 to give PEGylated ECO/*pDNA* nanoparticles. Excipient sucrose (5% or 10%) was added to the nanoparticle solution after nanoparticle formulation, and the whole solution was shaken for 15–30 min. The size and zeta potential of the nanoparticles were characterized by a dynamic light scattering (DLS) system (Litesizer 500; Anton Paar USA, Ashland, VA, USA).

In vitro transfection

ARPE-19 cells were cultured and pre-seeded onto 12-well plates (4×10^4 cells/well) and allowed to grow for 24 h at 37°C. Transfection was performed using medium with 10% serum, and the plasmid concentration of ECO/*pDNA* nanoparticles was set as 0.5 μg/mL. For the comparison experiment of ECO versus AAV2, ECO/*pCMV-GFP* nanoparticles were formulated at an N/P ratio of 8 with a pDNA concentration of 0.5 μg/mL in the transfection medium (ECO stock concentration of 5 mM and *pDNA* stock concentration of 0.5 μg/μL.). The amount of AAV2-pCMV-GFP (Vector Biosystems) was calculated to be the same as the plasmid concentration in the medium based on gene copy number. Cells were treated with ECO/*pCMV-GFP* and AAV2-pCMV-GFP for 4 h, and the transfection medium was replaced with fresh medium. Cells were incubated until 48 h. Flow cytometry was used to evaluate GFP expression after 48 h. Briefly, after removal of the culture medium, each well was washed twice with phosphate-buffered saline (PBS; 10 mM sodium phosphate [pH 7.2] containing 100 mM NaCl). Cells were harvested after treatment with 0.25% trypsin containing 0.26 mM EDTA (Invitrogen), followed by centrifugation at 1,500 rpm for 5 min and fixation in 500 μL PBS containing 4% paraformaldehyde, and finally passed through a 35-μm cell strainer (BD Biosciences). A BD FACSCalibur flow cytometer (BD Biosciences) was used to determine GFP expression based on the fluorescence intensity from a total of 10,000 cells for each sample.

Cytotoxicity

Potential cytotoxicity of ECO/*pABCA4* nanoparticles was investigated using a CCK-8 assay (Dojindo Molecular Technologies, Washington, DC, USA). Cell viability was evaluated using ARPE-19 cells on 96-well plates, where cells were seeded at a concentration of 1×10^4 cells per well. ARPE-19 cells were incubated with ECO/*pGRK1-ABCA4-SMAR* nanoparticles, PEGylated nanoparticles, or nanoparticles with sucrose (5%) at different DNA doses (12.5 ng, 25 ng, 50 ng, 100 ng, 200 ng, 400 ng, and 800 ng) in 100 μL DMEM (10% serum) for 4 h at 37°C. Then the nanoparticle-containing DMEM was replaced with fresh DMEM (10% serum). The cells were allowed to grow until 48 h, and then they were washed with PBS. CCK-8 reagent was added to each well, followed by incubation for 1.5 h at 37°C. The absorbance at 450 nm was recorded using a plate reader. Cell viability was calculated by normalizing to the absorption of a non-treated control.

In vivo transfection

Subretinal injection

Subretinal injection was adapted from the technical briefs described by Timmers et al.[50] and Johnson et al.[51]

For comparison of ECO/*pCMV-GFP* and AAV-pCMV-GFP, the genome copy number of injected AAV2-CMV-GFP was 5×10^9. The dose for *pCMV-GFP* was calculated to provide an amount of DNA equivalent to that for AAV2-CMV-GFP, which was 23 ng. EM-PEG-HZ-ECO/*pCMV-GFP* nanoparticles were formulated at N/P = 8 at a *pDNA* concentration of 46 ng/μL because our injection volume was one-half microliter. BALB/c mice (total of 10) were injected in one eye with ECO-based nanoparticles and in the other eye with AAV2 particles.

For evaluation of the effect of varying dosage on transfection efficiency, PEGylated (2.5% PEG) PEG-ECO/*pGRK1-ABCA4-S/MAR* nanoparticles were tested in *Abca4*$^{-/-}$ mice. PEG-ECO/*pGRK1-ABCA4-S/MAR* nanoparticles were formulated at N/P = 8 at a *pDNA* concentration of 50, 100, or 200 ng/μL. A total of 5 mice were injected in one eye with 0.5 μL of 50 ng/μL nanoparticles and in the contralateral eye with 0.5 μL of 100 ng/μL nanoparticles. Another 5 mice were injected in one eye with 0.5 μL of 100 ng/μL nanoparticles and in the contralateral eye with 0.5 μL of 200 ng/μL nanoparticles. Mice were injected at 5 weeks of age and sacrificed 1 week after injections. qRT-PCR was used for analysis of *ABCA4* mRNA expression.

For injection volume evaluation, PEGylated (2.5% PEG) PEG-ECO/*pGRK1-ABCA4-S/MAR* nanoparticles were tested in *Abca4*$^{-/-}$ mice. PEG-ECO/*pGRK1-ABCA4-S/MAR* nanoparticles were formulated at N/P = 8 at a *pDNA* concentration of 100 or 200 ng/μL. A total of 5 mice were injected in one eye with 1 μL of 100 ng/μL nanoparticles and in the contralateral eye with 0.5 μL of 200 ng/μL nanoparticles. Mice were injected at 6 weeks of age and sacrificed 1 week after injections. qRT-PCR was used for analysis of *ABCA4* mRNA expression.

For treatment age evaluation and gene expression time course study, PEGylated (2.5%) PEG-ECO/*pGRK1-ABCA4-S/MAR* nanoparticles were tested in *Abca4*$^{-/-}$ mice. PEGylated PEG-ECO/*pGRK1-ABCA4-S/MAR* nanoparticles were formulated at N/P = 8 at a *pDNA* concentration of 200 ng/μL as described previously. Groups

of mice were injected in both eyes with 0.5 μL of 200 ng/μL nanoparticles, at 5, 8, 12, 22, and 58 weeks of age, for evaluation of the effect of age. The mice were sacrificed 1 week after injections. qRT-PCR was used for analysis of *ABCA4* mRNA expression. For the time course study, a mixed population of mice (6–20 weeks old) was injected in both eyes using a standard formulation (PEG-ECO/*pGRK1-ABCA4-S/MAR*, N/P = 8, 200 ng/μL, 0.5 μL per eye); eyeballs were harvested at different time points (2 weeks, 1 month, 2 months, 3 months, 4 months, and 5 months). qRT-PCR was used for analysis of *ABCA4* mRNA expression.

For repeat-treatment experiments, $Abca4^{-/-}$ mice were divided into 3 groups and treated with PEGylated (2.5%) PEG-ECO/*pGRK1-ABCA4-S/MAR* nanoparticles (200 ng/μL). The inter-treatment interval was 3 months for repeated injections. $Abca4^{-/-}$ mice were treated with 0.5 μL of nanoparticles in both eyes. For the 1-treatment and 2-treatment groups, mice were sacrificed 8 months after the first treatment. For the 3-treatment group, mice were sacrificed 5 months after the third injection (11 months after the initial treatment).

Intravitreal injection

The injection was performed similarly as the subretinal injection. However, the nanoparticle solution was injected into the vitreous humor instead of the subretinal space. For evaluation of the injection route, 0.5 μL of nanoparticle solution was injected into the vitreous.

qRT-PCR

Tissues were homogenized manually using a Brinkmann Politron homogenizer (Kinematica, Lucerne, Switzerland) in the lysis buffer. RNA extraction was performed using a QIAGEN RNeasy kit. Then the mRNA transcripts were converted to cDNA using the SuperScript IV reverse transcriptase kit (Invitrogen). Finally, qRT-PCR was performed with SYBR Green Master Mix (AB Biosciences, Allston, MA, USA) in a Bio-Rad CFX96 real-time detection system. Fold changes were normalized to the 18S internal control, with non-treated or PBS-treated eyes as controls.

Electroretinography

Wild-type BALB/c mice and $Abca4^{-/-}$ mice were injected with PBS or ECO/*pGRK1-ABCA4-S/MAR* nanoparticles and PEGylated nanoparticles, as described above. Full-field ERGs were acquired according to a previous method.[52] BALB/c mice were evaluated 1 month after subretinal injections. The treated $Abca4^{-/-}$ mice (1 and 3 injections) were tested around 10 months after the first treatment.

SLO

In vivo whole-fundus and fluorescence imaging of mouse retinas of the treated and control mice at various time points was performed by SLO in infrared and autofluorescence modes (HRAII; Heidelberg Engineering, Heidelberg, Germany). Before imaging, mice were anesthetized by injection of a cocktail (10 μL/g body weight, intraperitoneally [i.p.]) of ketamine (6 mg/mL) and xylazine (0.44 mg/mL) in PBS and treated with 1% tropicamide for pupil dilation.

HPLC analysis of A2E

The A2E standard was synthesized and analyzed using HPLC as described previously.[18,19] A2E was eluted using gradients of ACN in water (containing 0.1% TFA), 40%–100% (15 min; flow rate, 1 mL/min), and the eluting peaks were monitored at 439 nm. The sample A2E peak was identified as the peak with the same elution time as the A2E standard. When the control group displayed 2 peaks for standard A2E with similar UV spectra, then the treatment groups were analyzed for both peaks.

Retina whole mount

Fresh harvested eyeballs were soaked in 10% formalin/PBS overnight and then washed with PBS several times. Under a dissection microscope, extra connective tissue was carefully removed by cutting with dissection scissors. Then the cornea was cut off, and the lens was squeezed out. Using two pairs of tweezers, choroid tissue was slowly torn off, leaving the retina untouched. Carefully, 4–5 cuts were made in the retina, and it was flattened. The flattened retina was transferred to a glass slide and adhered with mounting reagent.

IHC

Gene expression and distribution throughout the retina was studied using IHC. Briefly, histological slides were prepared by directly freezing the eyeballs collected from mice in OCT compound. Frozen slides were prepared with a thickness of 10 μm and adhered to glass slides. Prior to IHC, slides were warmed until they reached room temperature. Then the slides were washed in PBS with 0.5% Tween 20 (PBST). Fluorescein isothiocyanate (FITC)-labeled ABCA4 antibody (3F4 monoclonal) was purchased from Santa Cruz Biotechnology. Co-staining RPE65 antibody was purchased from Arigo Biolabs (catalog number ARG41875) and labeled with CF550 using antibody labeling kit (Biotium, catalog number 92254); these slides were imaged using a confocal microscope (FV1000; Olympus, Center Valley, PA, USA).

ELISA

Mice were sacrificed after single or multiple treatments. Blood was collected intracardially and allowed to stand at room temperature for 30 min before centrifugation at 5,000 rpm for 10 min. Serum was harvested into individual tubes and kept at −80°C until analysis. Mouse anti-PEG IgG and IgM ELISA kits were purchased from Life Diagnostics (catalog numbers PEGG-1 and PEGM-1). ELISA experiments were performed following the manufacturer's instructions. In brief, plates were provided with immobilized mono-mPEGylated BSA. A set of different concentrations of anti-PEG IgG/IgM was prepared and loaded to plates, respectively, as standards. Mouse serum samples (100 μL) were loaded onto plates in duplicates and incubated on a plate shaker at 150 rpm for 1 h at room temperature. Plates were washed 5 times with 400 μL of washing solution (provided in the kits). Horseradish peroxidase (HRP)-conjugated anti-mouse IgG/IgM (100 μL) was applied to each well and incubated on the shaker for 45 min. After 5 washes, 100 μL of TMB was dispensed into each well, and the plates were incubated for another 20 min before adding 100 μL of stop solution. Absorbance at 450 nm was measured on the

plate reader. A standard curve of IgG and IgM was plotted based on average readings from duplicated wells. The average reading from each sample was converted to IgG/IgM units according to a standard linear equation formula. Two tailed Fisher's t tests were analyzed for statistical significance.

Statistical analysis

The i*n vitro* experiments and *in vivo* animal treatments were performed at least in triplicate. The data are presented as the means and standard deviations. Statistical analysis was conducted with ANOVA and two-tailed Student's t tests using a 95% confidence interval. Statistical significance was accepted when $p \leq 0.05$.

SUPPLEMENTAL INFORMATION

Supplemental information can be found online at https://doi.org/10.1016/j.omtn.2022.08.026.

ACKNOWLEDGMENTS

This project was supported by the Gund-Harrington Scholars Award from the Harrington Discovery Institute and the Foundation Fighting Blindness, National Cancer Institute R01CA235152, and unrestricted grants from Research to Prevent Blindness to the Departments of Ophthalmology at the University of California Irvine. K.P. is a Donald Bren Professor and Irving H. Leopold Chair of Ophthalmology. Z.-R.L. is an M. Frank Rudy and Margaret Domiter Rudy Professor of Biomedical Engineering.

AUTHOR CONTRIBUTIONS

Z.-R.L., D.S. and W.S. conceived the strategy and designed the experiments. D.S. and W.S. were involved in all aspects of this work. W.S., D.S., and S.L. performed subretinal injections. S.-Q.G. performed ERG examinations. J.L., C.W., and A.N. performed nanoparticle analysis. A.L.S. and J.S. performed ECO synthesis. R.C.H. assisted with data analysis. E.I.T. and K.P. provided animal models and assisted with experiment design. All authors read and approved the final manuscript.

DECLARATION OF INTERESTS

The gene therapy reported in this work was licensed to Helios BioPharmaceuticals for commercialization. Z.-R.L. may have ownership interest in the company.

REFERENCES

1. Boye, S.E., Boye, S.L., Lewin, A.S., and Hauswirth, W.W. (2013). A comprehensive review of retinal gene therapy. Mol. Ther. *21*, 509–519.
2. Allikmets, R., Shroyer, N.F., Singh, N., Seddon, J.M., Lewis, R.A., Bernstein, P.S., Peiffer, A., Zabriskie, N.A., Li, Y., Hutchinson, A., et al. (1997). Mutation of the Stargardt disease gene (ABCR) in age-related macular degeneration. Science *277*, 1805–1807.
3. Tsybovsky, Y., Molday, R.S., and Palczewski, K. (2010). The ATP-binding cassette transporter ABCA4: structural and functional properties and role in retinal disease. Adv. Exp. Med. Biol. *703*, 105–125.
4. Molday, R.S., Garces, F.A., Scortecci, J.F., and Molday, L.L. (2022). Structure and function of ABCA4 and its role in the visual cycle and Stargardt macular degeneration. Prog. Retin. Eye Res. *89*, 101036.
5. Gardiner, K.L., Cideciyan, A.V., Swider, M., Dufour, V.L., Sumaroka, A., Komáromy, A.M., Hauswirth, W.W., Iwabe, S., Jacobson, S.G., Beltran, W.A., and Aguirre, G.D. (2020). Long-term structural outcomes of late-stage RPE65 gene therapy. Mol. Ther. *28*, 266–278.
6. Boye, S.L., Peterson, J.J., Choudhury, S., Min, S.H., Ruan, Q., McCullough, K.T., Zhang, Z., Olshevskaya, E.V., Peshenko, I.V., Hauswirth, W.W., et al. (2015). Gene Therapy Fully Restores Vision to the All-Cone Nrl$^{(-/-)}$ Gucy2e$^{(-/-)}$ Mouse Model of Leber Congenital Amaurosis-1. Hum. Gene Ther. *26*, 575–592.
7. Russell, S., Bennett, J., Wellman, J.A., Chung, D.C., Yu, Z.-F., Tillman, A., Wittes, J., Pappas, J., Elci, O., McCague, S., et al. (2017). Efficacy and safety of voretigene neparvovec (AAV2-hRPE65v2) in patients with RPE65-mediated inherited retinal dystrophy: a randomised, controlled, open-label, phase 3 trial. Lancet *390*, 849–860.
8. Lipinski, D.M., Thake, M., and MacLaren, R.E. (2013). Clinical applications of retinal gene therapy. Prog. Retin. Eye Res. *32*, 22–47.
9. Lin, G.Z., Yang, J.T., Wei, S.C., Chen, S.E., Huo, S.D., and Ma, Z.R. (2018). Immunogenicity of adenovirus and DNA vaccines co-expressing P39 and lumazine synthase proteins of Brucella abortus in BALB/c mice. Trop. Anim. Health Prod. *50*, 957–963.
10. Annoni, A., Gregori, S., Naldini, L., and Cantore, A. (2019). Modulation of immune responses in lentiviral vector-mediated gene transfer. Cell. Immunol. *342*, 103802.
11. Nidetz, N.F., McGee, M.C., Tse, L.V., Li, C., Cong, L., Li, Y., and Huang, W. (2020). Adeno-associated viral vector-mediated immune responses: understanding barriers to gene delivery. Pharmacol. Ther. *207*, 107453.
12. Sun, D., Sahu, B., Gao, S., Schur, R.M., Vaidya, A.M., Maeda, A., Palczewski, K., and Lu, Z.-R. (2017). Targeted multifunctional lipid ECO plasmid DNA nanoparticles as efficient non-viral gene therapy for Leber's congenital amaurosis. Mol. Ther. Nucleic Acids *7*, 42–52.
13. Sun, D., Maeno, H., Gujrati, M., Schur, R., Maeda, A., Maeda, T., Palczewski, K., and Lu, Z.-R. (2015). Self-assembly of a multifunctional lipid with core–shell dendrimer DNA nanoparticles enhanced efficient gene delivery at low charge ratios into RPE cells. Macromol. Biosci. *15*, 1663–1672.
14. Sun, D., Sun, Z., Jiang, H., Vaidya, A.M., Xin, R., Ayat, N.R., Schilb, A.L., Qiao, P.L., Han, Z., Naderi, A., and Lu, Z.R. (2019). Synthesis and evaluation of pH-sensitive multifunctional lipids for efficient delivery of CRISPR/Cas9 in gene editing. Bioconjug. Chem. *30*, 667–678.
15. Vaidya, A.M., Sun, Z., Ayat, N., Schilb, A., Liu, X., Jiang, H., Sun, D., Scheidt, J., Qian, V., He, S., et al. (2019). Systemic delivery of tumor-targeting siRNA nanoparticles against an oncogenic LncRNA facilitates effective triple-negative breast cancer therapy. Bioconjug. Chem. *30*, 907–919.
16. Dinculescu, A., Glushakova, L., Min, S.H., and Hauswirth, W.W. (2005). Adeno-associated virus-vectored gene therapy for retinal disease. Hum. Gene Ther. *16*, 649–663.
17. Ayat, N.R., Sun, Z., Sun, D., Yin, M., Hall, R.C., Vaidya, A.M., Liu, X., Schilb, A.L., Scheidt, J.H., and Lu, Z.-R. (2019). Formulation of biocompatible targeted ECO/siRNA nanoparticles with long-term stability for clinical translation of RNAi. Nucleic Acid Ther. *29*, 195–207.
18. Sun, D., Schur, R.M., Sears, A.E., Gao, S.-Q., Vaidya, A., Sun, W., Maeda, A., Kern, T., Palczewski, K., and Lu, Z.-R. (2020). Non-viral gene therapy for Stargardt disease with ECO/pRHO-ABCA4 self-assembled nanoparticles. Mol. Ther. *28*, 293–303.
19. Sun, D., Sun, W., Gao, S.-Q., Wei, C., Naderi, A., Schilb, A.L., Scheidt, J., Lee, S., Kern, T.S., Palczewski, K., and Lu, Z.R. (2021). Formulation and efficacy of ECO/pRHO-ABCA4-SV40 nanoparticles for nonviral gene therapy of Stargardt disease in a mouse model. J. Control. Release *330*, 329–340.
20. Argyros, O., Wong, S.P., Niceta, M., Waddington, S.N., Howe, S.J., Coutelle, C., Miller, A.D., and Harbottle, R.P. (2008). Persistent episomal transgene expression in liver following delivery of a scaffold/matrix attachment region containing non-viral vector. Gene Ther. *15*, 1593–1605.
21. Young, J.E., Vogt, T., Gross, K.W., and Khani, S.C. (2003). A short, highly active photoreceptor-specific enhancer/promoter region upstream of the human Rhodopsin kinase gene. Invest. Ophthalmol. Vis. Sci. *44*, 4076–4085.
22. Koirala, A., Makkia, R.S., Conley, S.M., Cooper, M.J., and Naash, M.I. (2013). S/MAR-containing DNA nanoparticles promote persistent RPE gene expression and improvement in RPE65-associated LCA. Hum. Mol. Genet. *22*, 1632–1642.

23. Koirala, A., Conley, S.M., and Naash, M.I. (2014). Episomal maintenance of S/MAR-Containing non-viral vectors for RPE-based diseases. In Retinal Degenerative Diseases, J.D. Ash, C. Grimm, J.G. Hollyfield, R.E. Anderson, M.M. LaVail, and C.B. Rickman, eds. (Springer), pp. 703–709.

24. Koirala, A., Conley, S.M., Makkia, R., Liu, Z., Cooper, M.J., Sparrow, J.R., and Naash, M.I. (2013). Persistence of non-viral vector mediated RPE65 expression: Case for viability as a gene transfer therapy for RPE-based diseases. J. Control. Release *172*, 745–752.

25. Han, Z., Conley, S.M., and Naash, M.I. (2014). Gene therapy for Stargardt disease associated with ABCA4 gene. In Retinal Degenerative Diseases, J.D. Ash, C. Grimm, J.G. Hollyfield, R.E. Anderson, M.M. LaVail, and C.B. Rickman, eds. (Springer), pp. 719–724.

26. Wang, Y., Rajala, A., Cao, B., Ranjo-Bishop, M., Agbaga, M.-P., Mao, C., and Rajala, R.V.S. (2016). Cell-specific promoters enable lipid-based nanoparticles to deliver genes to specific cells of the retina in vivo. Theranostics *6*, 1514–1527.

27. Radu, R.A., Mata, N.L., Bagla, A., and Travis, G.H. (2004). Light exposure stimulates formation of A2E oxiranes in a mouse model of Stargardt's macular degeneration. Proc. Natl. Acad. Sci. USA *101*, 5928–5933.

28. Kennedy, C.J., Rakoczy, P.E., and Constable, I.J. (1995). Lipofuscin of the retinal pigment epithelium: a review. Eye *9*, 763–771.

29. Radu, R.A., Mata, N.L., Nusinowitz, S., Liu, X., Sieving, P.A., and Travis, G.H. (2003). Treatment with isotretinoin inhibits lipofuscin accumulation in a mouse model of recessive Stargardt's macular degeneration. Proc. Natl. Acad. Sci. USA *100*, 4742–4747.

30. Radu, R., Mata, N., Sieving, P., and Travis, G. (2002). Treatment of abcr$^{-/-}$ mice with isotretinoin inhibits accumulation of lipofuscin. Investig. Ophthalmol. Vis. Sci. *43*, 4579.

31. Kubota, R., Birch, D.G., Gregory, J.K., and Koester, J.M. (2022). Randomised study evaluating the pharmacodynamics of emixustat hydrochloride in subjects with macular atrophy secondary to Stargardt disease. Br. J. Ophthalmol. *106*, 403–408.

32. Charbel Issa, P., Barnard, A.R., Herrmann, P., Washington, I., and MacLaren, R.E. (2015). Rescue of the Stargardt phenotype in Abca4 knockout mice through inhibition of vitamin A dimerization. Proc. Natl. Acad. Sci. USA *112*, 8415–8420.

33. Julien-Schraermeyer, S., Illing, B., Tschulakow, A., Taubitz, T., Guezguez, J., Burnet, M., and Schraermeyer, U. (2020). Penetration, distribution, and elimination of remofuscin/soraprazan in Stargardt mouse eyes following a single intravitreal injection using pharmacokinetics and transmission electron microscopic autoradiography: implication for the local treatment of Stargardt's disease and dry age-related macular degeneration. Pharmacol. Res. Perspect. *8*, e00683.

34. Kong, J., Kim, S.R., Binley, K., Pata, I., Doi, K., Mannik, J., Zernant-Rajang, J., Kan, O., Iqball, S., Naylor, S., et al. (2008). Correction of the disease phenotype in the mouse model of Stargardt disease by lentiviral gene therapy. Gene Ther. *15*, 1311–1320.

35. Binley, K., Widdowson, P., Loader, J., Kelleher, M., Iqball, S., Ferrige, G., de Belin, J., Carlucci, M., Angell-Manning, D., Hurst, F., et al. (2013). Transduction of photoreceptors with equine infectious anemia virus lentiviral vectors: safety and biodistribution of StarGen for Stargardt disease. Invest. Ophthalmol. Vis. Sci. *54*, 4061–4071.

36. Trapani, I., Toriello, E., de Simone, S., Colella, P., Iodice, C., Polishchuk, E.V., Sommella, A., Colecchi, L., Rossi, S., Simonelli, F., et al. (2015). Improved dual AAV vectors with reduced expression of truncated proteins are safe and effective in the retina of a mouse model of Stargardt disease. Hum. Mol. Genet. *24*, 6811–6825.

37. McClements, M.E., Barnard, A.R., Singh, M.S., Charbel Issa, P., Jiang, Z., Radu, R.A., and MacLaren, R.E. (2019). An AAV dual vector strategy ameliorates the Stargardt phenotype in adult Abca4$^{(-/-)}$ mice. Hum. Gene Ther. *30*, 590–600.

38. Tornabene, P., Trapani, I., Minopoli, R., Centrulo, M., Lupo, M., de Simone, S., Tiberi, P., Dell'Aquila, F., Marrocco, E., Iodice, C., et al. (2019). Intein-mediated protein trans-splicing expands adeno-associated virus transfer capacity in the retina. Sci. Transl. Med. *11*, eaav4523.

39. Cideciyan, A.V., Jacobson, S.G., Beltran, W.A., Sumaroka, A., Swider, M., Iwabe, S., Roman, A.J., Olivares, M.B., Schwartz, S.B., Komáromy, A.M., et al. (2013). Human retinal gene therapy for Leber congenital amaurosis shows advancing retinal degeneration despite enduring visual improvement. Proc. Natl. Acad. Sci. USA *110*, E517–E525.

40. Mingozzi, F., and High, K.A. (2011). Immune responses to AAV in clinical trials. Curr. Gene Ther. *11*, 321–330.

41. Corbett, K.S., Edwards, D.K., Leist, S.R., Abiona, O.M., Boyoglu-Barnum, S., Gillespie, R.A., Himansu, S., Schäfer, A., Ziwawo, C.T., DiPiazza, A.T., et al. (2020). SARS-CoV-2 mRNA vaccine design enabled by prototype pathogen preparedness. Nature *586*, 567–571.

42. Mulligan, M.J., Lyke, K.E., Kitchin, N., Absalon, J., Gurtman, A., Lockhart, S., Neuzil, K., Raabe, V., Bailey, R., Swanson, K.A., et al. (2020). Phase I/II study of COVID-19 RNA vaccine BNT162b1 in adults. Nature *586*, 589–593.

43. Gujrati, M., Malamas, A., Shin, T., Jin, E., Sun, Y., and Lu, Z.-R. (2014). Multifunctional cationic lipid-based nanoparticles facilitate endosomal escape and reduction-triggered cytosolic siRNA release. Mol. Pharm. *11*, 2734–2744.

44. Gujrati, M., Vaidya, A., and Lu, Z.-R. (2016). Multifunctional pH-sensitive amino lipids for siRNA delivery. Bioconjug. Chem. *27*, 19–35.

45. Malamas, A.S., Gujrati, M., Kummitha, C.M., Xu, R., and Lu, Z.-R. (2013). Design and evaluation of new pH-sensitive amphiphilic cationic lipids for siRNA delivery. J. Control. Release *171*, 296–307.

46. Sun, D., Schur, R.M., Sears, A.E., Gao, S.-Q., Sun, W., Naderi, A., Kern, T., Palczewski, K., and Lu, Z.-R. (2020). Stable retinoid analogue targeted dual pH-sensitive smart lipid ECO/pDNA nanoparticles for specific gene delivery in the retinal pigment epithelium. ACS Appl. Bio Mater. *3*, 3078–3086.

47. Yin, H., Kanasty, R.L., Eltoukhy, A.A., Vegas, A.J., Dorkin, J.R., and Anderson, D.G. (2014). Non-viral vectors for gene-based therapy. Nat. Rev. Genet. *15*, 541–555.

48. Maeda, A., Maeda, T., Golczak, M., and Palczewski, K. (2008). Retinopathy in mice induced by disrupted all-trans-retinal clearance. J. Biol. Chem. *283*, 26684–26693.

49. Schilb, A.L., Scheidt, J.H., Vaidya, A.M., Sun, Z., Sun, D., Lee, S., and Lu, Z.R. (2021). Optimization of synthesis of the amino lipid ECO for effective delivery of nucleic acids. Pharmaceuticals *14*, 1016.

50. Timmers, A.M., Zhang, H., Squitieri, A., and Gonzalez-Pola, C. (2001). Subretinal injections in rodent eyes: effects on electrophysiology and histology of rat retina. Mol. Vis. *7*, 131–137.

51. Johnson, C.J., Berglin, L., Chrenek, M.A., Redmond, T.M., Boatright, J.H., and Nickerson, J.M. (2008). Technical brief: subretinal injection and electroporation into adult mouse eyes. Mol. Vis. *14*, 2211–2226.

52. Schur, R.M., Sheng, L., Sahu, B., Yu, G., Gao, S., Yu, X., Maeda, A., Palczewski, K., and Lu, Z.-R. (2015). Manganese-enhanced MRI for preclinical evaluation of retinal degeneration treatments. Invest. Ophthalmol. Vis. Sci. *56*, 4936–4942.

OMTN, Volume *29*

Supplemental information

Effective gene therapy of Stargardt disease with PEG-ECO/*pGRK1-ABCA4-S/MAR* nanoparticles

Da Sun, Wenyu Sun, Song-Qi Gao, Jonathan Lehrer, Amirreza Naderi, Cheng Wei, Sangjoon Lee, Andrew L. Schilb, Josef Scheidt, Ryan C. Hall, Elias I. Traboulsi, Krzysztof Palczewski, and Zheng-Rong Lu

SUPPLEMENTARY INFORMATION

Effective Gene Therapy of Stargardt Disease with PEG-ECO/*pGRK1-ABCA4-S/MAR* Nanoparticles

1. Construction of *ABCA4* plasmid DNA with the human *GRK1* promoter, human beta-Globin *polyA* and human *S/MAR* enhancer.

Previously, we have demonstrated excellent efficacy using our ECO-based gene therapy platform involving a therapeutic plasmid with a bovine rhodopsin promoter and an enhancer with viral origin [1, 2]. Here, a new *ABCA4* plasmid DNA with a human promoter and enhancer has been constructed to promote specific expression of ABCA4 in both cone and rod photoreceptors for possible clinical use. A DNA fragment of the human *GRK1* (-109 to + 183) promoter and a beta-Globin *polyA* were amplified from human genomic DNA, according to a previous work [3]. A human scaffold/matrix attachment region enhancer (*S/MAR*) DNA was also incorporated in the plasmid construct to enhance/prolong gene expression. The *GRK1* promoter was inserted into *MluI* and *AgeI* restriction sites, while the *polyA* and *S/MAR* DNA were inserted into *NotI* and *NheI* restriction sites. The whole plasmid maps of *pGRK1-ABCA4-S/MAR* and control plasmids *pRHO-ABCA4* and *pGRK1-ABCA4 without S/MAR* are shown in **Fig. S1A**. The respective plasmid structures were confirmed by digestion with multiple restriction enzymes and agarose gel electrophoresis (**Fig. S1B)**. Four restriction enzymes, *MluI, AgeI*, *NotI* and *NheI*, were used in multiple enzyme digestion reactions. Agarose gel (1%) was prepared to separate 4 DNA fragments after digestion. In this new therapeutic plasmid, promoter *GRK1* (300 bp), *ABCA4* (6.8 kb), *polyA*+*S/MAR* (2.9 kb) and vector backbone (~2.5 kb) were separated after digestion and gel electrophoresis. While building the therapeutic construct, we further deleted some non-essential sequences from vector and reduced size of vector backbone to 2.5 kb. The electrophoresis results confirmed the success of plasmid construction. Full length sequencing was also performed on the new *ABCA4* plasmid.

After modification, a similar *ABCA4* expression level in *Abca4*$^{-/-}$ mice was observed with the *GRK1* promoter as with the *RHO* promoter (**Fig. S1C)**. The addition of the *S/MAR* enhancer facilitated similar *ABCA4* mRNA expression 1 week after treatment, compared to without

S/MAR. However, significantly prolonged expression was observed 1 month after treatment, compared to no enhancer control, demonstrating gene expression enhancement effect for a longer time (**Fig. S1D)**.

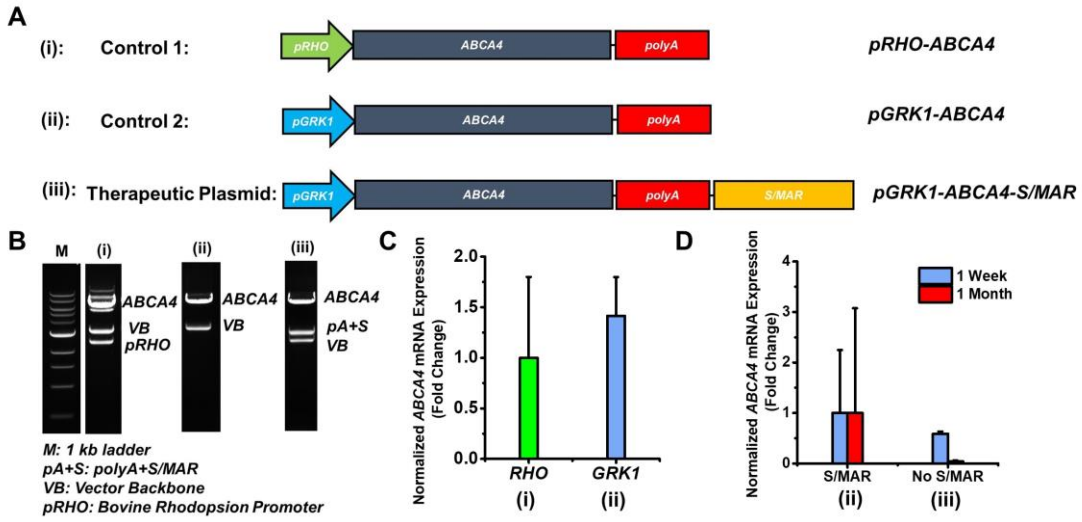

Fig. S1. Therapeutic plasmid construction, structure confirmation, and characterization of expression. (A) Diagram of functional components, **(B)** agarose gel electrophoresis of multiple restriction-enzyme digestion to verify correct-sized DNA fragments of (i) control pRHO-ABCA4; (ii) pGRK1-ABCA4; and (iii) therapeutic *pGRK1-ABCA4-SMAR*. The *GRK1* promoter was inserted between *MluI* and *AgeI* restriction sites. *ABCA4* mRNA expression in *Abca4*$^{-/-}$ mice 1 week or 1 month after subretinal administration of ECO/pDNA nanoparticles (100 ng/eye), using plasmids with different promoters **(C)** (i) and (ii); or **(D)** with (ii) and without(iii) *S/MAR* enhancer modification.

2. Characterization of ECO/*pGRK1-ABCA4-S/MAR* nanoparticles

All the ECO/*pDNA* nanoparticle formulations were formulated as described in the materials and methods section. Sucrose (10%) was added to the nanoparticle solution after formulation. The sizes and zeta potentials were evaluated also as described in the materials and methods section. Agarose gel electrophoresis was used to evaluate the encapsulation and stability of the formulations of ECO/*pGRK1-ABCA4-S/MAR* nanoparticles, either fresh made or under different storage conditions (4℃ and -20 ℃). Encapsulated DNA will reduce mobility

when nanoparticles are formed. Specifically, 4 formulations were tested: **(i)** ECO/*pGRK1-ABCA4-S/MAR,* **(ii)** ECO/*pGRK1-ABCA4-S/MAR* (10% sucrose) **(iii)** PEG-ECO/*pGRK1-ABCA4-S/MAR,* and **(iv)** PEG-ECO/*pGRK1-ABCA4-S/MAR* (10% sucrose). Results are displayed in **Fig. S2.** All the nanoparticles demonstrated efficient *pDNA* encapsulation and excellent stability for 1 week and 1 month after storage at 4℃ or -20 ℃, indicated by the bright bands on the top of each agarose electrophoresis gel (**Fig. S2)**.

Dynamic light scattering (DLS) of size distributions from the formulations of ECO/*pGRK1-ABCA4-S/MAR* nanoparticles were summarized in **Fig. S2D**. **(i)** ECO/*pGRK1-ABCA4-S/MAR* nanoparticles demonstrated good stability until aggregations formation after a month storage under -20 ℃, where a wider size distribution was shown. There was no significant change in the size distribution observed for **(ii)** ECO/*pGRK1-ABCA4-S/MAR* (10% sucrose)*,* **(iii)** PEG-ECO/*pGRK1-ABCA4-S/MAR* and **(iv)** PEG-ECO/*pGRK1-ABCA4-S/MAR* (10% sucrose) nanoparticles **Fig. S2D**. The sizes and zeta potentials are summarized also in **Table S1.** All the nanoparticle formulations demonstrated consistent sizes (150 nm~200 nm) and proper positive zeta potentials (+15 mV~45 mV). The effect of storage on expression was also evaluated. No change was observed after 45 days of storage of the same nanoparticle formulation, and significant transfection efficiency was retained for the formulation after storage at -20℃ for 70 days (**Fig. S2E)**.

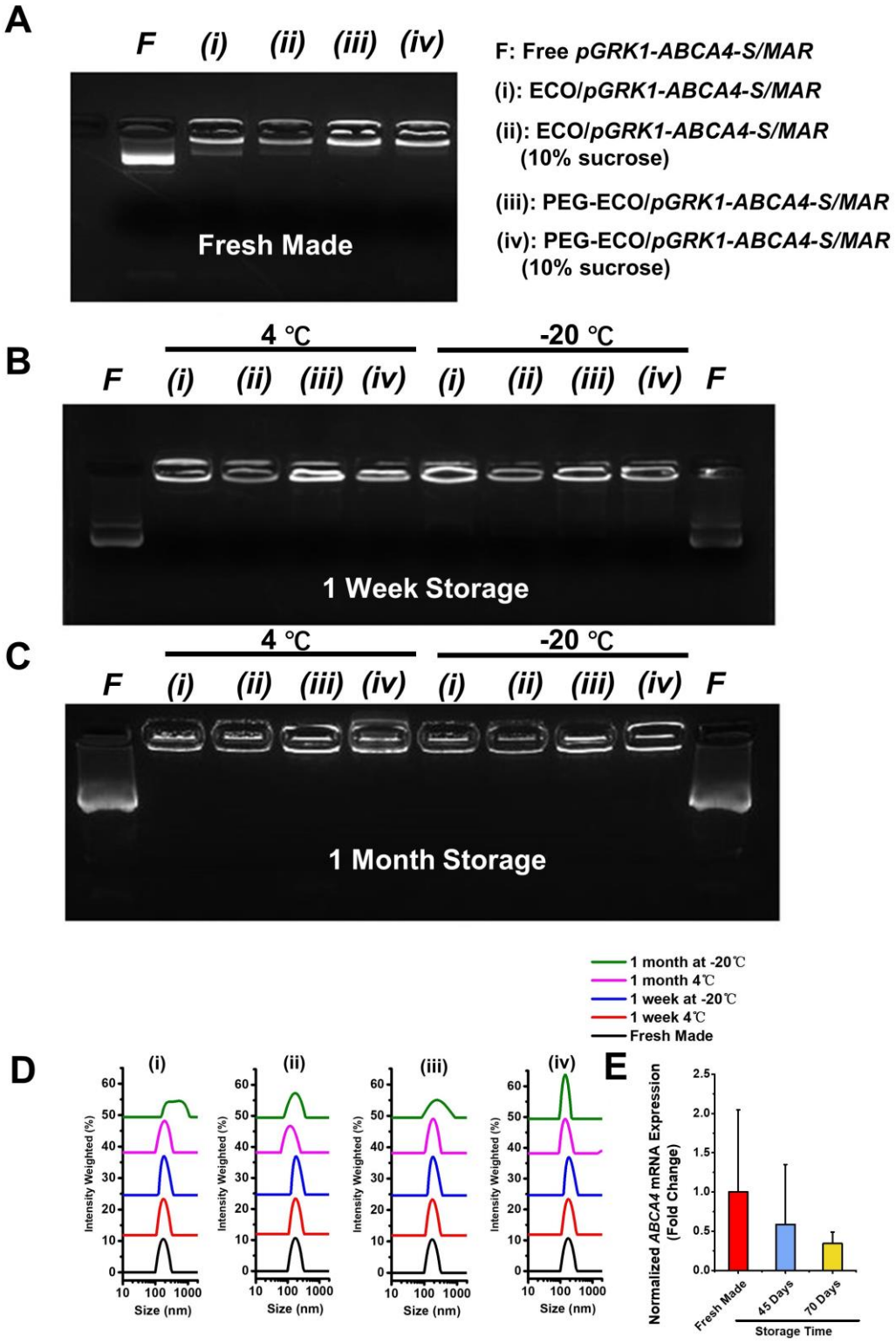

Fig. S2. Stability of ECO/*pGRK1-ABCA4-S/MAR* nanoparticle formulations. (A,B,C) Agarose gel electrophoresis and **(D)** nanoparticle size distribution of (i) ECO/*pGRK1-ABCA4-S/MAR,* (ii) ECO/*pGRK1-ABCA4-S/MAR* (10% sucrose), (iii) PEG-ECO/*pGRK1-ABCA4-S/MAR* and (iv) PEG-ECO/*pGRK1-ABCA4-S/MAR* (10% sucrose) nanoparticles under storage condition of 4 ℃ or -20 ℃ at day 0 (fresh made), day 7 and 1 month; **(E)** *ABCA4* mRNA

expression by qRT-PCR analysis of *Abca4*$^{-/-}$ mice treated with PEG-ECO/*pGRK1-ABCA4-S/MAR* (5% sucrose) nanoparticles (100 ng/eye) stored at -20℃ for 45 or 70 days. **(A)** is also shown in **Figure 1E**.

Table S1. Sizes and zeta potentials of ECO/*pGRK1-ABCA4-S/MAR* nanoparticle formulations

	Particle Size (nm)				
Formulations	**0 day**	**7 day 4℃**	**7 day -20℃**	**1 month day 4℃**	**1 month day -20℃**
ECO/*pGRK1-ABCA4-S/MAR*	186.46	199.43	200.5	198.8	427
PEG-ECO/*pGRK1-ABCA4-S/MAR*	189.74	189.12	210.5	200	211
ECO/*pGRK1-ABCA4-S/MAR* (10% Sucrose)	151.15	173.71	186.6	125.79	173.92
PEG-ECO/*pGRK1-ABCA4-S/MAR* (10% Sucrose)	174.06	182.53	174.67	175.28	171.11
	Zeta Potential (mV)				
Formulations	**0 day**	**7 day 4℃**	**7 day -20℃**	**1 month day 4℃**	**1 month day -20℃**
ECO/*pGRK1-ABCA4-S/MAR*	21.8	26.4	40.3	30.4	44.6
PEG-ECO/*pGRK1-ABCA4-S/MAR*	13.8	15.1	22.5	30.4	28.6
ECO/*pGRK1-ABCA4-S/MAR* (10% Sucrose)	21.9	25.5	49.8	39.8	45
PEG-ECO/*pGRK1-ABCA4-S/MAR* (10% Sucrose)	15.7	23	17.7	27.7	18.7

3. HPLC Analysis of A2E with sample chromatograms from mice received single treatment of different doses and multi-treatments.

A2E, composed of photo-toxic dimers of vitamin A, is a main component of lipofuscin [4, 5]. A2E accumulation is commonly used as an indicator of STGD progression [6]. One of the therapeutic strategies for treating STGD is to slow down the production and accumulation of A2E to minimize chronic oxidative damage that ultimately leads to atrophy. A2E accumulation gradually increased in *Abca4*$^{-/-}$ mice with aging, as has been demonstrated in our previous research [1]. A2E analysis was performed as described in the methods. The HPLC chromatograms were used to quantify relative A2E diminution compared with untreated controls. The area of the A2E peak was integrated and the peaks for treated mice were normalized to the peaks of control mice. The HPLC chromatograms are summarized for mice treated with a single dose (50 ng or 100 ng/eye) of PEG-ECO/*pGRK1-ABCA4-S/MAR* nanoparticles, **Fig. S3** (4 months after treatment), **Fig. S4 (**8 months after treatment), and **Fig. S5** (1 year after treatment).

For multiple treatments, the HPLC chromatograms are summarized in **Fig. S6** for mice treated with a single dose (100 ng/eye), 2 doses (2×100 ng/eye, at a3 months interval) or 3 doses (3×100 ng/eye, at 3 month intervals) of PEG-ECO/*pGRK1-ABCA4-S/MAR* nanoparticles. From the chromatograms, smaller A2E peaks could be observed in the treated groups *versus*

the control groups, especially for the multiple treatment groups. The quantitative analysis was presented in the manuscript **Fig. 2G** and **Fig. 3F**.

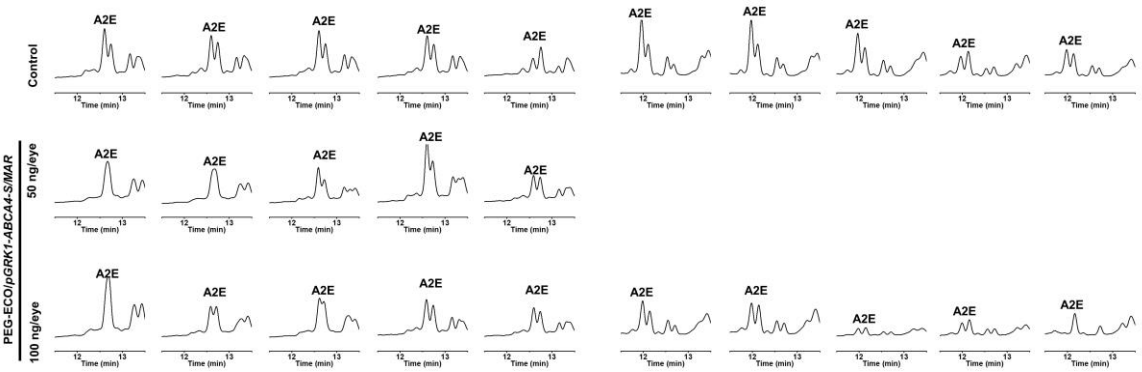

Fig. S3. Four months efficacy of PEG-ECO/ *pGRK1-ABCA4-S/MAR* nanoparticles for preventing A2E accumulation in *Abca4*$^{-/-}$ mice. HPLC chromatograms showing A2E peaks from control and nanoparticle-treated *Abca4*$^{-/-}$ mice 4 months after a single dose (50 ng or 100 ng/eye) of PEG-ECO/ *pGRK1-ABCA4-S/MAR* nanoparticles.

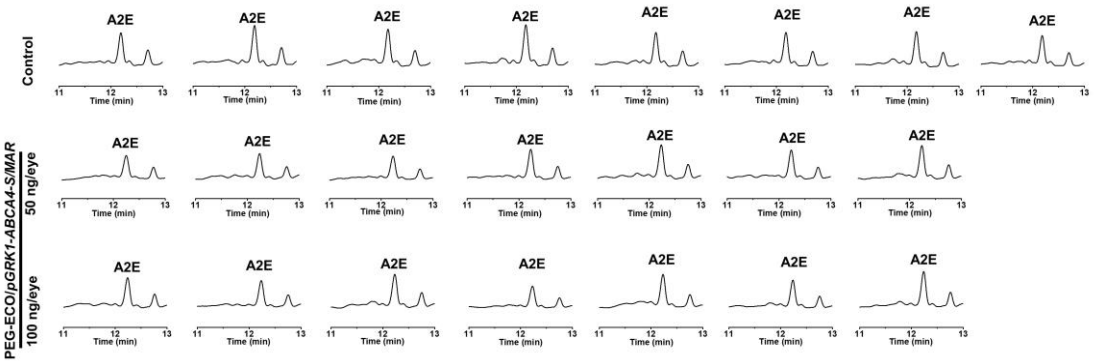

Fig. S4. Eight month efficacy of PEG-ECO/ *pGRK1-ABCA4-S/MAR* nanoparticles for preventing A2E accumulation in *Abca4*$^{-/-}$ mice. HPLC chromatograms showing A2E peaks from control and nanoparticle-treated *Abca4*$^{-/-}$ mice 8 months after a single dose (50 ng or 100 ng/eye) of PEG-ECO/ *pGRK1-ABCA4-S/MAR* nanoparticles.

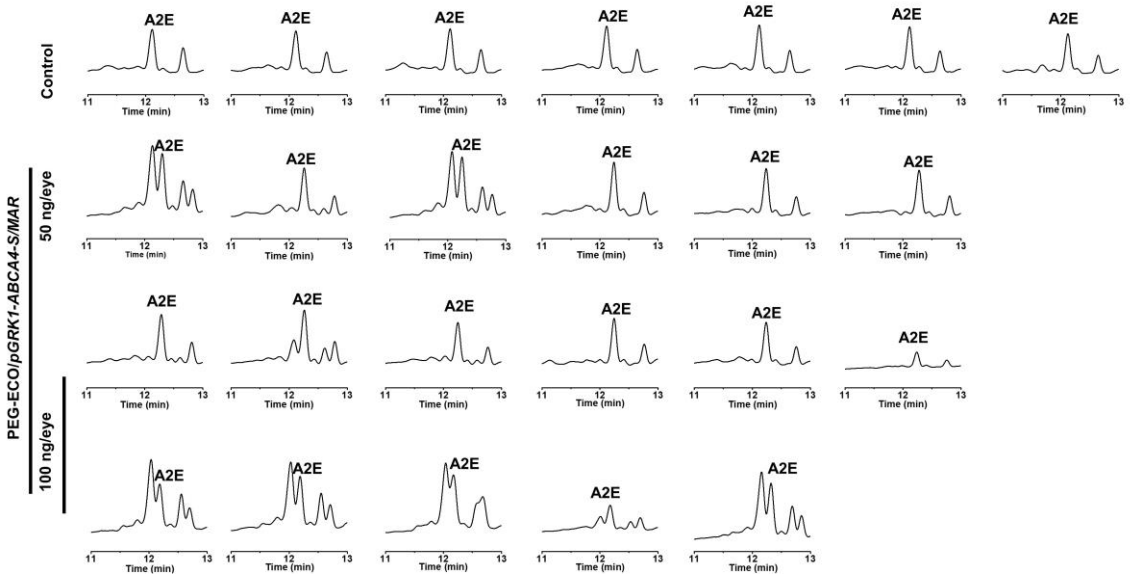

Fig. S5. One year efficacy of PEG-ECO/ *pGRK1-ABCA4-S/MAR* nanoparticles for preventing A2E accumulation in *Abca4*$^{-/-}$ mice. HPLC chromatograms showing A2E peaks from control and nanoparticle-treated *Abca4*$^{-/-}$ mice 1 year after a single dose (50 ng or 100 ng/eye) of PEG-ECO/ *pGRK1-ABCA4-S/MAR* nanoparticles.

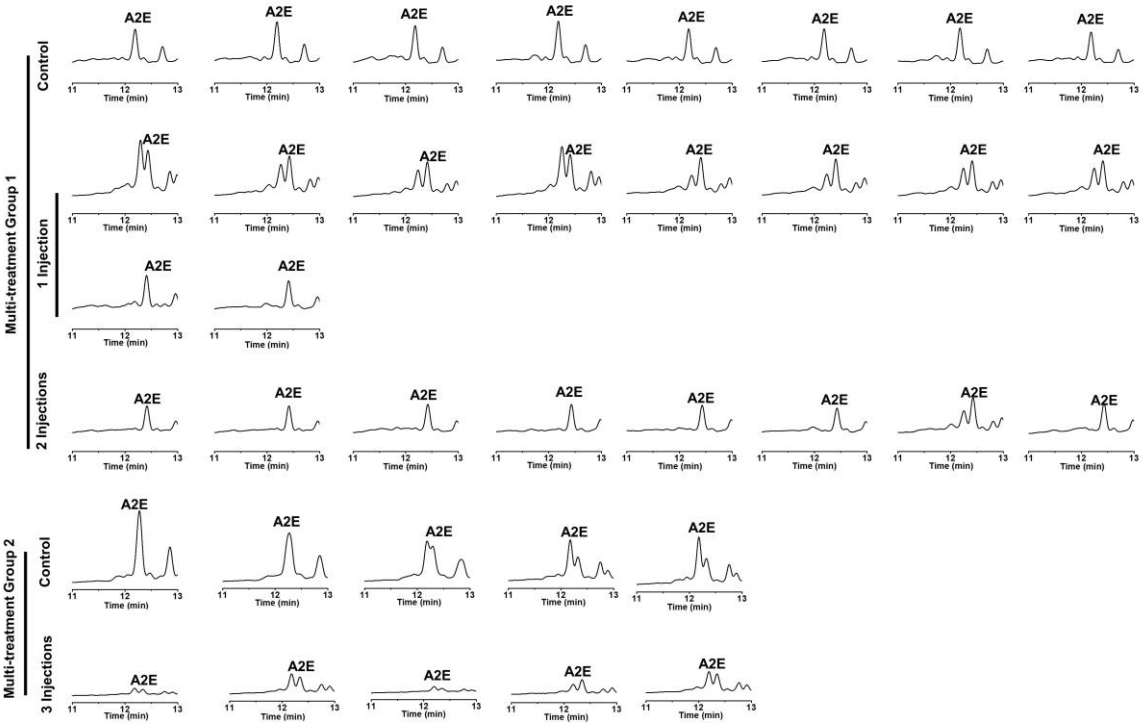

Fig. S6. Efficacy demonstrated by inhibition of A2E accumulation after multiple treatments with PEG-ECO/*pGRK1-ABCA4-S/MAR* nanoparticles (at 3 month intervals, 100 ng/eye). HPLC chromatograms showing A2E peaks from control and nanoparticle treated *Abca4*$^{-/-}$ mice.

Mice with 1 injection were sacrificed 8 months after injection; mice with 2 injections were sacrificed 5 months after the 2nd injection (8 months after the initial treatment); and mice with 3 injections were sacrificed 5 months after the 3rd injection.

The amount of A2E in the retinas of *Abca4*$^{-/-}$ mice after multi-treatments are summarized in **Fig. S7**. The quantification was based on HPLC analysis of A2E standard with a known concentration.

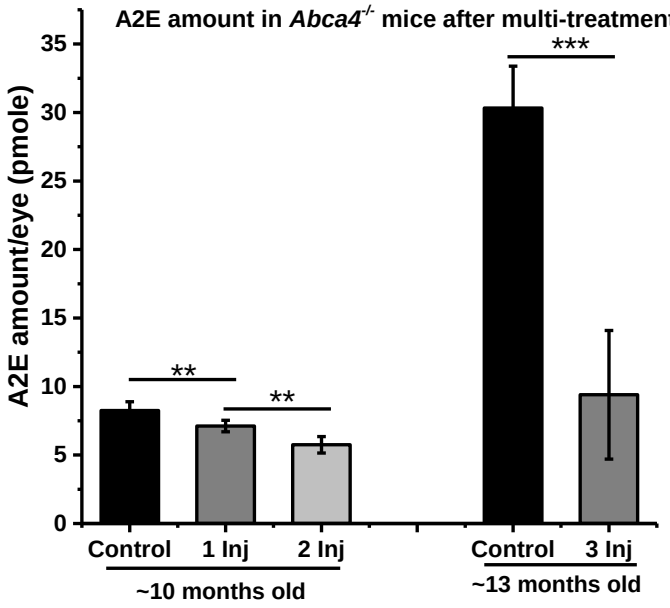

Figure S7. A2E amount (pmoles/eye) in the eyes of *Abca4*$^{-/-}$ mice after multi-treatments of gene therapy using PEG-ECO/*pGRK1-ABCA4-S/MAR* nanoparticles (every 3 months, 100 ng/eye). Mice with 1 injection were sacrificed 8 months after injection, mice with 2 injections were sacrificed 5 months after the 2nd injection (8 months after the initial treatment), the mice age was around 10 months when analyzed; Mice with 3 injections were sacrificed 5 months after the 3rd injection, the mice age was around 13 months when analyzed (** $p < 0.01$; ***$p<0.005$).

4. Safety of PEG-ECO/*pGRK1-ABCA4-S/MAR* nanoparticles

The cytotoxicity of ECO/*pGRK1-ABCA4-S/MAR* and PEG-ECO/*pGRK1-ABCA4-S/MAR* nanoparticles was first evaluated *in vitro* in ARPE-19 cells. Briefly, ECO/*pGRK1-ABCA4-S/MAR* nanoparticles were formulated at N/P ratios of 6 and 8 (see methods for detailed procedures). The nanoparticles were also tested after PEGylation using 2.5 mol% PEG, or

addition of 5% sucrose separately at an N/P ratio of 8. The cytotoxicity of ECO/*pGRK1-ABCA4-S/MAR* nanoparticles was evaluated at different *pDNA* doses (800 ng, 400 ng, 200 ng, 100 ng, 50 ng, 25 ng, 12.5 ng in 100 µL of transfection media) in ARPE-19 cells. ARPE-19 cells were seeded on a 96-well plate at 10,000 cells/well. Cells were treated with ECO/*pGRK1-ABCA4-S/MAR* and ECO/*pGRK1-ABCA4-S/MAR* (with 2.5 mol% PEG or 5% sucrose) nanoparticles for 4 hr, and the transfection medium was replaced with fresh medium. Cells were further incubated until 48 hr after transfection. The CCK-8 assay was used to evaluate cell viability after 48hr. The results are summarized in **Fig. S8.** ECO/*pGRK1-ABCA4-S/MAR* nanoparticles demonstrated dose-dependent cytotoxicity; for most doses of both N/P ratios, the nanoparticle formulations displayed low toxicity. Also, the N/P=6 formulation seemed to have lower cytotoxicity compared with N/P=8 (**Fig. S8A**). When PEGylation (2.5 mol% PEG) or 5% sucrose was incorporated into ECO/*pGRK1-ABCA4-S/MAR* nanoparticles, no obvious cytotoxicity was observed for the formulations across all the doses at N/P=8 **(Fig. S8B)**.

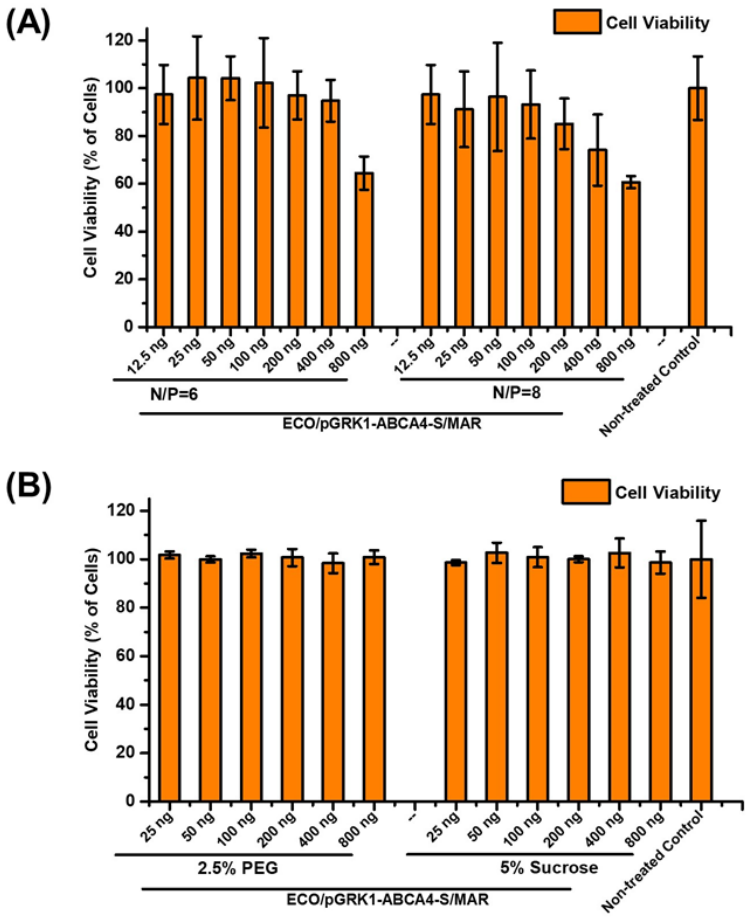

Fig. S8. *In vitro* cytotoxicity of the formulations of ECO/*pGRK1-ABCA4-S/MAR* nanoparticles. Cytotoxicity assessed by ARPE-19 cell viability 48 hr after transfection with ECO/*pGRK1-ABCA4-S/MAR* nanoparticles at N/P ratios of 6 and 8 **(A)** and with ECO/*pGRK1-ABCA4-S/MAR* nanoparticles formulated at N/P = 8 in 2.5% PEG or 5% sucrose **(B)**. Transfections were performed with *pDNA* doses of 800, 400, 200, 100, 50, 25, and 12.5 ng/100 µL media.

In vivo safety was evaluated using scotopic and photopic electroretinogram (ERG) responses after treatment with ECO/*pGRK1-ABCA4-S/MAR* in wild type *BALB/c* mice. A total of 5 *BALB/c* mice were injected with ECO/*pGRK1-ABCA4-S/MAR* nanoparticles formulated at a N/P=8 and a *pDNA* concentration of 200 ng/µL. The nanoparticles (0.5 µL) were injected into the subretinal space of the right eye, and 0.5 µL of PBS was injected to the left eye as the control. The mice were evaluated 1 month after injection by both scotopic and photopic electroretinogram (ERG). Results are summarized in **Fig. S9**.

After subretinal injection of ECO/*pGRK1-ABCA4-S/MAR* nanoparticles, *BALB/c* mice displayed similar ERG responses with similar intensities for both particles and PBS control, across all the tested light intensities; all mice also did not display any changes in the waveforms (**Fig. S9**). Therefore, ECO/*pGRK1-ABCA4-S/MAR* nanoparticles demonstrated good *in vivo* safety and mild to no adverse effects to eye function 1 month after a single injection in wild type *BALB/c* mice.

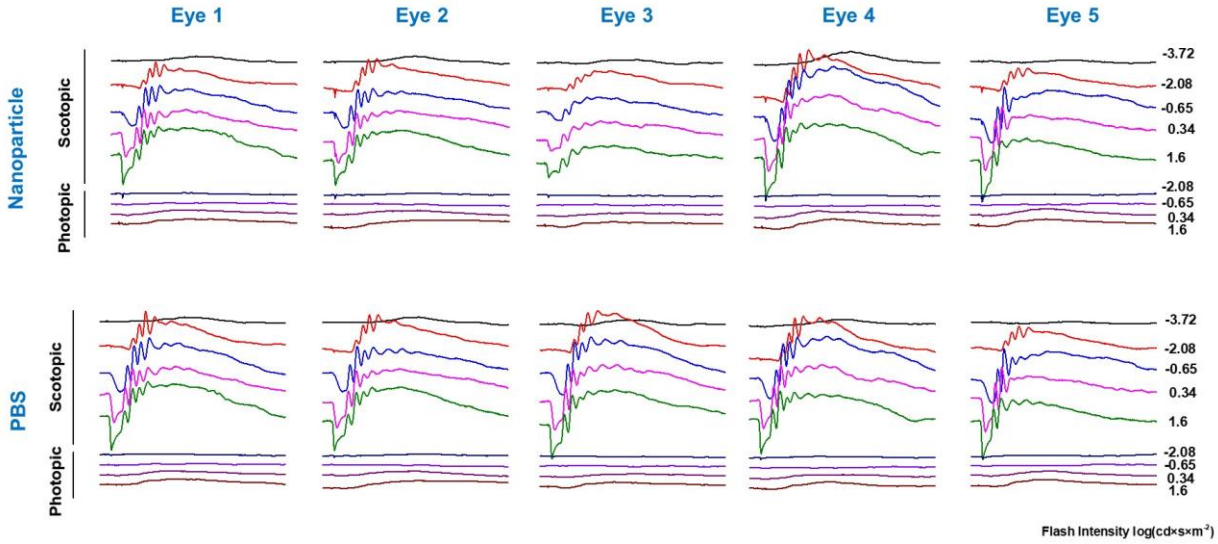

Fig. S9. Functional scotopic and photopic electroretinogram (ERG) analysis of *BALB/c* mice 1 month after subretinal injection of ECO/*pGRK1-ABCA4-S/MAR* nanoparticles at the test light intensities of -3.72~1.6 log(cd×s×m^{-2}).

Electroretinography (ERG) was also used to evaluate the eye function of *Abca4*$^{-/-}$ mice 10~10.5 months after the initial treatment, to assess the safety of treatment with PEG-ECO/*pGRK1-ABCA4-S/MAR* nanoparticles at a single dose (100 ng/eye) or 3 doses (3×100 ng/eye). Results are summarized in **Fig. S10**. No differences were observed in the ERG scotopic and photopic responses at the test intensity of 1.6 log(cd×s×m^{-2}) compared with the untreated control mice **(Fig. S10)**. Therefore, PEG-ECO/*pGRK1-ABCA4-S/MAR* nanoparticles demonstrated good *in vivo* safety both for single dose treatment and multiple treatments of *Abca4*$^{-/-}$ mice.

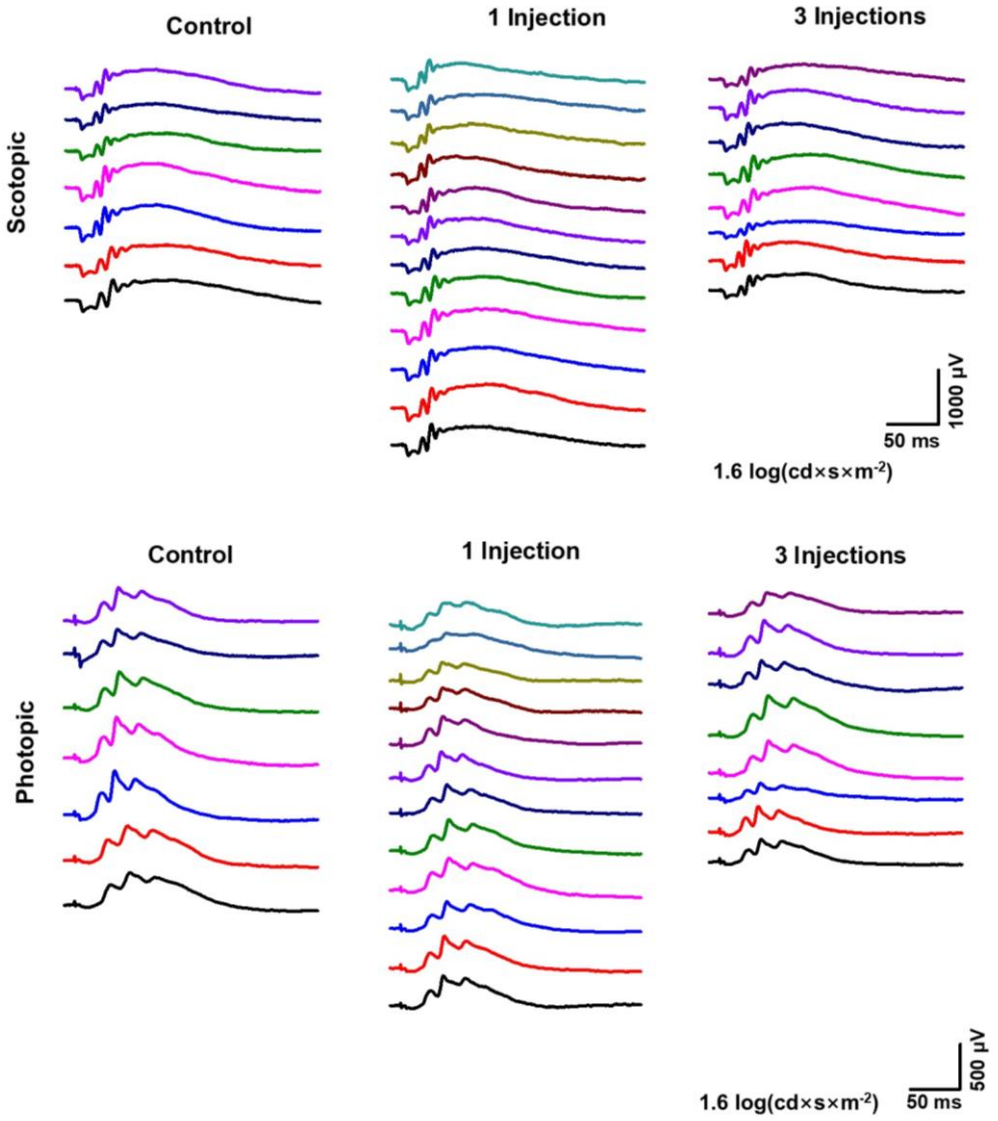

Fig. S10. Functional scotopic and photopic electroretinogram (ERG) analysis of *Abca4*$^{-/-}$ mice 10~10.5 months after the initial subretinal injection of 1 dose (100 ng/eye) or 3 doses (100 ng/eye at 3 month intervals) of PEG-ECO/*pGRK1-ABCA4-S/MAR* nanoparticles at the test light intensity of 1.6 log(cd×s×m^{-2}).

Using SLO in the fluorescent mode, we evaluated the morphology of the eyes of *Abca4*$^{-/-}$ mice 7 months after their initial treatment with multiple doses of ECO platform-based GRT using PEG-ECO/*pGRK1-ABCA4-S/MAR* nanoparticles. Results are summarized in **Fig. S11**. No treatment-associated adverse effects were observed for the 1-dose or 2-dose treatments compared with untreated control. Mice that received 3 doses seemed to have some injection-associated detachments (dark areas); however, these mice were tested only one month after the 3rd injection, so these detachments could have recovered if assessed at a later time.

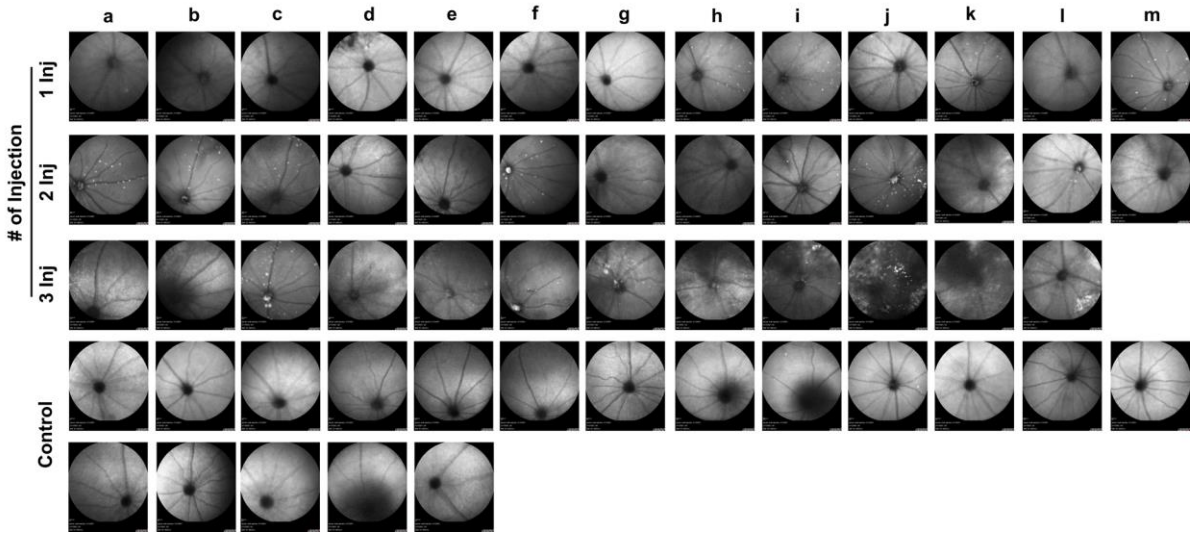

Fig. S11. Safety of PEG-ECO/*pGRK1-ABCA4-S/MAR* nanoparticles. Eye morphology was assessed 7 months after the first subretinal treatment (control: untreated) by fluorescent-scanning laser ophthalmoscopy (SLO), and fluorescent images are shown for *Abca4*$^{-/-}$ mice that received multiple doses of PEG-ECO/*pGRK1-ABCA4-S/MAR* nanoparticles. Mice were treated at 3 month intervals. SLO was performed 7 months after the initial injection (4 months after the 2nd injection, and 1 month after the 3rd injection). Selected SLO images are also shown in **Figure 4C**.

In vivo safety of the ECO/*pDNA* nanoparticles was also evaluated by morphology of the eye in comparison with AAV2. Briefly, ACU-PEG-HZ-ECO/*pCMV-GFP* nanoparticles (the ACU ligand was used to enhance interphotoreceptor matrix delivery) were formulated at N/P = 8 at a *pDNA* concentration of 46 ng/uL with 5% sucrose. The nanoparticles (0.5 uL) were injected into the subretinal space of one eye of a *BALB/c* mouse. The contralateral eye was injected with AAV2-CMV-GFP at an equivalent dose (calculated based on GFP copy number). Untreated mice were used as controls. Scanning laser ophthalmoscope (SLO, fluorescent mode) was used to evaluate the eye condition at 1, 2 and 3 months post injection using the fluorescent mode. Results are summarized in **Fig. S12**. AAV2 seemed to induce more lesions and potential inflammations than ECO nanoparticles, as demonstrated by the saturated white color regions. These results demonstrated the ECO/*pDNA* nanoparticles to have a potentially better safety profile.

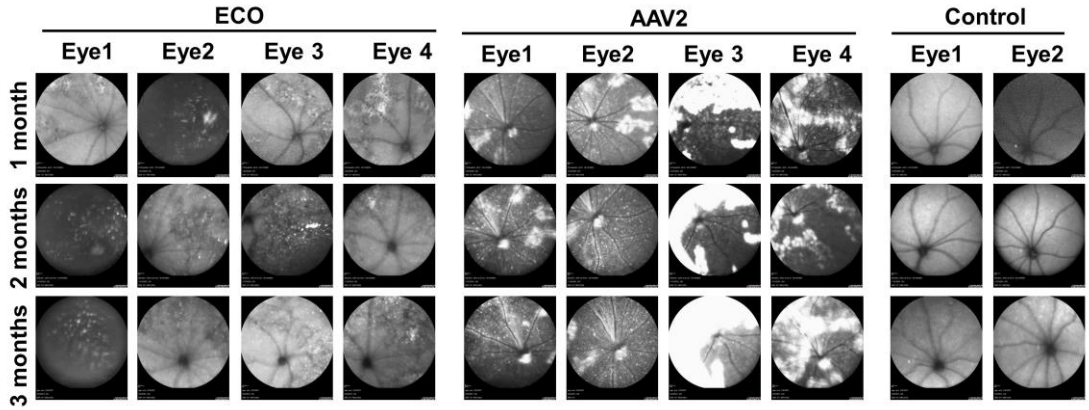

Fig. S12. Safety of EM-PEG-HZ-ECO/*pCMV-GFP* nanoparticles compared with AAV2 viral particles. Eye morphology of *BALB/c* mice treated with EM-PEG-HZ-ECO/*pCMV-GFP* nanoparticles or AAV2-CMV-GFP *versus* control (untreated) was assessed by fluorescent scanning laser ophthalmoscope (SLO) images of the eye 1, 2 and 3 months after treatments (all treated mice received the same dose by gene copy number). Selected SLO images are also shown in **Figure 4D**.

Table S2. Primer information

Name	Sequence 5'-3'
ABCA4 qPCR Forward	TCCAAGCACCTCCAGTTTATC
ABCA4 qPCR Reverse	CCCAGCACTCACGGAATAAT
18s internal control Forward	AGGATCCATTGGAGGGCAAGT
18s internal control Reverse	TCCAACTACGAGCTTTTTAACTGCA
ABCA4 genotyping Forward	TCTCGGGGATGTTTTGAGAC
ABCA4 genotyping Reverse	AATGGATCCACACCACCAAC
NEO-F	CGTTGGCTACCCGTGATATT
pGRK1 Forward	GGGCCCCAGAAGCCTGGTGGTTGTTTGTCCTTCTCAGG
pGRK1 Reverse	GCCCTTGCCTGTGGCCCGTCCCTGCCCTTGCTGG
MluI insertion Forward	CCGAAAAGTGCCACCTGACGCGTCGACATTGATTATTGAC
MluI insertion Reverse	GTCAATAATCAATGTCGACGCGTCAGGTGGCACTTTTCGG
NheI insertion Forward	AAGGCCGCGTTGCTAGCGTTTTTCCATAGGC
NheI insertion Reverse	GCCTATGGAAAAACGCTAGCAACGCGGCCTT
Globin polyA Forward	ACATTTGCTTCTGACACAACTGTGTTCACTAGCAACCTC
Globin polyA Reverse	GCAATGAAAATAAATGTTTTTTATTAGGCAGAATCCAGATGCTCAAGG
S/MAR Forward	TGCAACACCCCAGTAAAGAG
S/MAR Reverse	TAGCTAGCTCTATCAAGATATTTAAAGAAAAAAAAAATTGTATCAACTTTATACAATCTC

Reference

1. Sun, D, Schur, RM, Sears, AE, Gao, S-Q, Vaidya, A, Sun, W*, et al.* (2020). Non-viral Gene Therapy for Stargardt Disease with ECO/pRHO-ABCA4 Self-Assembled Nanoparticles. *Molecular Therapy* **28**: 293-303.
2. Sun, D, Sun, W, Gao, S-Q, Wei, C, Naderi, A, Schilb, AL*, et al.* (2021). Formulation and efficacy of ECO/pRHO-ABCA4-SV40 nanoparticles for nonviral gene therapy of Stargardt disease in a mouse model. *Journal of Controlled Release* **330**: 329-340.
3. Young, JE, Vogt, T, Gross, KW, and Khani, SC (2003). A Short, Highly Active Photoreceptor-Specific Enhancer/Promoter Region Upstream of the Human Rhodopsin Kinase Gene. *Investigative Ophthalmology & Visual Science* **44**: 4076-4085.
4. Radu, RA, Mata, NL, Bagla, A, and Travis, GH (2004). Light exposure stimulates formation of A2E oxiranes in a mouse model of Stargardt's macular degeneration. *Proceedings of the National Academy of Sciences of the United States of America* **101**: 5928-5933.
5. Kennedy, CJ, Rakoczy, PE, and Constable, IJ (1995). Lipofuscin of the retinal pigment epithelium: A review. *Eye* **9**: 763.
6. Radu, RA, Mata, NL, Nusinowitz, S, Liu, X, Sieving, PA, and Travis, GH (2003). Treatment with isotretinoin inhibits lipofuscin accumulation in a mouse model of recessive Stargardt's macular degeneration. *Proceedings of the National Academy of Sciences* **100**: 4742-4747.